

EFFECT OF SINTERING IN OXYGEN DEFICIENT ATMOSPHERE ON ZrO_2 WITH CaO

By

PARVATI RAMASWAMY



MATERIALS SCIENCE PROGRAMME

INDIAN INSTITUTE OF TECHNOLOGY KANPUR
AUGUST, 1984

EFFECT OF SINTERING IN OXYGEN DEFICIENT ATMOSPHERE ON ZrO_2 WITH CaO

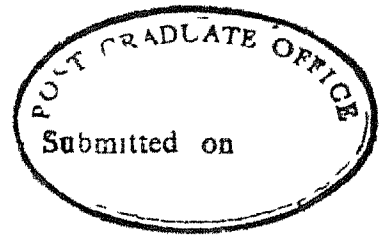
A Thesis Submitted
in Partial Fulfilment of the Requirements
for the Degree of
MASTER OF TECHNOLOGY

1984

By
PARVATI RAMASWAMY

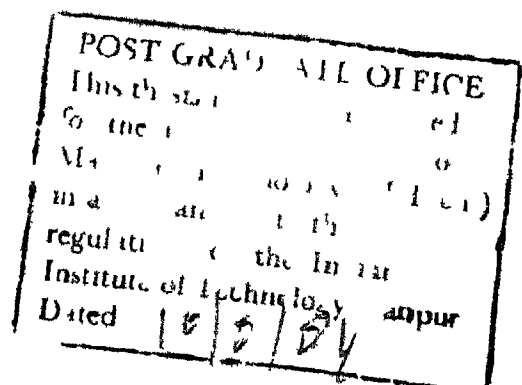
to the

MATERIALS SCIENCE PROGRAMME
INDIAN INSTITUTE OF TECHNOLOGY KANPUR
AUGUST, 1984



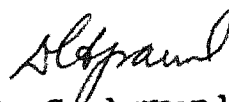
TO

Patta, Chittammai, Appai and Immi



CERTIFICATE

This is to certify that this work on "The Effect of Sintering in Oxygen Deficient Atmosphere on ZrO_2 with CaO " by Parvati Ramaswamy has been carried out under my supervision and that this has not been submitted elsewhere for a degree



D. C. Agrawal
Assistant Professor
Materials Science Programme
Indian Institute of Technology
Kanpur

1
2
3
4
5
6
7
8
9
10
11
12
13
14
15
16
17
18
19
20
21
22
23
24
25
26
27
28
29
30
31
32
33
34
35
36
37
38
39
40
41
42
43
44
45
46
47
48
49
50
51
52
53
54
55
56
57
58
59
60
61
62
63
64
65
66
67
68
69
70
71
72
73
74
75
76
77
78
79
80
81
82
83
84
85
86
87
88
89
90
91
92
93
94
95
96
97
98
99
100

ACKNOWLEDGEMENTS

I acknowledge with gratitude my debt to Dr D C Agrawal for his excellent guidance and for being a constant source of inspiration at each and every stage of my work

I am extremely grateful to Dr K Shahi for providing me with all facilities for conductivity measurements

I also wish to acknowledge my appreciation to all those staff of the Advance Centre of Materials Science who assisted me in the preparation of this report. I am particularly grateful to Mr. B Sharma, Mr B K Jain, Mr V P Sharma, Mr S Das and Mr U Singh

The cordiality and companionship of all my friends at I I T Kanpur is sincerely appreciated. Special thanks are due to Mr R N Srivastava for his skilful typing of the manuscript

PARVATI RAMASWAMY

CONTENTS

	ABSTRACT	vii
CHAPTER I	INTRODUCTION	1
CHAPTER II	SAMPLE PREPARATION	7
CHAPTER III	PHASE ANALYSIS	10
CHAPTER IV	MICROSTRUCTURE ANALYSIS	33
CHAPTER V	CONDUCTIVITY MEASUREMENTS	47
CHAPTER VI	DENSITY AND POROSITY MEASUREMENTS	54
CHAPTER VII	: CHANGES ON REOXIDATION	61
CHAPTER VIII	MECHANICAL PROPERTIES	69
CHAPTER IX	CONCLUSIONS	74
	REFERENCES	77
	APPENDIX	79

ABSTRACT

Samples of zirconia containing 0, 4, 8 and 15 mole % of calcia were sintered at 1900°C in $\sim 10^{-11}$ atmos partial pressure oxygen. Analysis were performed on phases, microstructure, conductivity, mechanical properties and reoxidation behaviour.

Phase analysis was carried out by X-ray diffraction and transmission electron microscopy. X-ray diffraction analysis showed that the samples without calcia additive contained both monoclinic and cubic phases while samples containing 8 mole % calcia were completely stabilized in the cubic fluorite defect structure. Transmission electron microscopy gave evidence for the presence of zirconium metal in samples containing 8 and 15 mole % calcia respectively.

Microstructure by scanning electron microscopy also indicated the presence of zirconium metal in the form of discrete particles in the samples containing 8 and 15 mole % of calcia respectively.

All samples had turned black or grey in colour indicating presence of large anion vacancy concentration. The conductivity of samples containing 0, 4 and 8 mole % calcia respectively increases with increase in temperature, reaches a maximum and then drops before rising again with further increase in temperature. It is suggested that this may be a result of removal of the excess oxygen ion vacancies.

The as sintered samples were reoxidized in air and their phases were analysed by X-ray diffraction. All the samples were found to have become white in colour indicating entry of oxygen ions in the lattice. Destabilization was found to be more at about 1000°C than at 1350°C. This is believed to be due to the destructive effect of the Tetragonal \Rightarrow Monoclinic transformation temperature. The samples heat treated at 1350°C were found to retain their shape without crumbling while most of the samples were found to have disintegrated to fine particles on heat treatment at 1000°C. Samples of all compositions gained weight on reoxidation at 1300°C which increased with increase in calcia content in the samples.

Measurements of microhardness indicated the DPH numbers of C_8 and C_{15} to be much larger than those of C_0 and C_{15} . This is believed to arise partly due to the higher hardness of the cubic phase as compared to the monoclinic phase and partly due to the presence of large number of anion vacancies.

CHAPTER I

INTRODUCTION

The chemistry of zirconia has attracted the attention of both the theoretical scientist and the practical industrialist interested in high temperature materials. Zirconia is one of the most refractory oxides, its melting point being $2680^{\circ}\text{C} \pm 20^{\circ}\text{C}$ [1]. Apart from possessing high degree of corrosion resistance it also possesses, high strength and modulus and attractive electrical transport properties. It finds wide applications in heat exchange furnaces [2], crucibles and pouring nozzles for molten metals, furnace linings, solid electrolyte in fuel cells and oxygen sensors and bushings for glass fibre drawing etc.

Although zirconia has excellent refractive properties, its use in bulk form is restricted by the destructive tetragonal \rightleftharpoons monoclinic phase transformation which occurs at $\approx 1000^{\circ}\text{C}$ [3]. Thermal cycling through the transformation range ($800^{\circ}\text{C} \rightleftharpoons 1200^{\circ}\text{C}$) causes cracking and sometimes complete disintegration of sintered specimens because a volume change of 3% accompanies transformation. Therefore interest has centered on 'alloys' of ZrO_2 with other oxides (CaO , MgO , Y_2O_3) primarily because these oxides can form stable solid solutions with the cubic fluorite structure at room temperature which is its high temperature polymorphic form at 2370°C .

Cubic zirconia stabilized with divalent or trivalent oxides is a nonstoichiometric substance with defect fluorite structure, the defects being anion vacancies. The general formula is $M_xZr_{1-x}O_{2-x}$. The properties of the material (such as melting point, thermal expansion and electrical conductivity) are functions of the compositional parameter x [4]. On addition of MO , the M^{2+} (cation) replaces a Zr^{4+} and an anion vacancy is created in order to maintain charge neutrality. The defect concentration increases with addition of the stabilizer and generally about 12 mole % of CaO is needed to obtain a single phase stabilized material [5]. Fully stabilized cubic zirconia is not particularly resistant to thermal shock, but partially stabilized zirconia (PSZ) can be both stronger and more resistant to thermal shock than either unstabilized or fully stabilized bodies [3]. Furthermore, the complete stability of FSZ is somewhat in question. Many of the cubic zirconia are destabilized (monoclinic ZrO_2 exsolution) by long annealing treatment near the destructive monoclinic \rightleftharpoons tetragonal inversion temperature. The improved properties of the PSZ are the result of its microstructure which can be controlled by the amount of stabilizer added and heat treatment.

The improved thermal shock resistance and mechanical properties of PSZ are believed to arise due to the extensive microcracking during transformation of monoclinic phase. Because of their large numbers, these cracks propagate only quasi-statically and the body maintains a large portion of its strength after continuous thermal cycling [6].

Porter et al. [7] explained the improved fracture toughness of PSZ on the basis of transformation toughening of the tetragonal particles on interaction with the stress field of a propagating crack. This is done by their martensitic transformation to monoclinic structure and absorption of energy. Thus, it has been confirmed that PSZ have superior mechanical and thermal properties over FSZ

Several investigators have carried out experiments on zirconia which is deficit in oxygen. Such materials have been prepared by sintering either pure zirconia or zirconia with metal or carbon additions in low partial pressures of oxygen. It was their intention to observe if zirconia with or without any additives attained any significant effects on its basic properties due to oxygen deficiency.

Johnson [8] reported that zirconia samples heated above 1600°C in vacuum turned almost black. The combination ZrO_2 -carbon, sintered in vacuum at 1600°C reduced ZrO_2 to nonstoichiometric ZrO_{2-x} and formed zirconium carbide at higher temperature. When they were heated to temperature above 2100°C , an increase in hardness and strength with no cracking was observed. No evidence of decomposition of ZrO_2 to metallic Zr was shown by X-ray analysis which indicated lack of decomposition.

Fehrenbacher et.al. [9] sintered ZrO_2 bars in a tantalum resistance vacuum furnace at $2000^{\circ}\text{C}/20$ hrs. They attributed the resultant black appearance of the samples to oxygen deficiency. Test conducted in air at around 1100°C resulted in oxidation of the ZrO_2 bars or powders as evidenced

by transition to a white colour

Harold Garrett and Rubert Ruh [10] also report that ZrO_2 specimens sintered in a vacuum induction furnace at 2300°C for three hours operating at 10^{-4} torr or lower produced sound, black oxygen deficient zirconia. Reoxidation in air resulted in disintegration of samples. It was believed that environmental gradients as well as temperature and oxidation rates contributed to the reoxidation problem. It was also believed that density gradients in uniaxially pressed specimens contributed to the disintegration of reoxidized specimens. These assumptions were based on observation of structural integrity, warping and the predominance of micro-cracks normal to the pressing direction.

Carniglia et.al. [11] report that zirconia samples sintered in vacuum at $2100^\circ\text{C}/1.3 \times 10^{-7}$ atmosphere show thin grain boundary films and small inclusions which are largely discontinuous and randomly scattered throughout the specimen. Electron microprobe and selected area diffraction analysis identified the phase as Zr metal. Free Zr was observed only at the lowest O_2 partial pressure used (10^{-7} atm) and only in that portion of the specimen heated above 1800°C .

X-ray diffraction show the volume of the O deficient material to be slightly less than that of the stoichiometric material. The two phase (as sintered) zirconia contained ≈ 0.09 wt % Zr metal, the static Young's modulus and tensile strength of which disclosed no major differences attributable to O deficiency. Reoxidation at 1000°C resulted in oxidation of the grain boundary phase at this temperature which

destroyed the integrity of the structure. However, the metal phase present in the vacuum sintered ZrO_2 was found to be uniquely associated with marked thermal stress resistant quality.

Robert Ruh et al [12] studied the diffusion of titanium into ZrO_2 from a vapour source on firing at $2000^\circ\text{C}/3$ hrs in vacuum. The reduced zirconia at the outer edge of the sample was found to be so oxygen deficient that it contained free Zr in the grain boundaries. However, no explanation was given by them for this large oxygen deficiency at the edges of the diffusion sample.

Weber et.al [13] have attributed the blackness of zirconia heated in vacuo at temperature $>2100^\circ\text{C}$ to the solid solution of zirconium in zirconia the air annealing of which at high temperature $\approx 1000^\circ\text{C}$ leads to their rapid oxidation and consequent disintegration.

Walter Tripp and Norman M Tallan [14] report very small weight change for ZrO_2 discs sintered at 2000°C in vacuum and reoxidized in air at 800°C for 24 hrs. Weight change over a O_2 partial pressure range of 10^{-1} to 10^{-11} atmosphere never exceeded $\approx 10 \mu\text{g}$. However, large weight changes have been observed by Carniglia et al when black ZrO_2 produced by extensive reduction is reoxidized. Walter Tripp et.al. [14] suggested that the weight changes observed in black ZrO_2 might indicate either defect structure changes at much lower O_2 pressure or oxidation of free metal present in the specimens.

Thus, it may be concluded from the observations of other workers that zirconia sintered at high temperature ($>1800^{\circ}\text{C}$) in low partial pressure of oxygen resulted in black, oxygen deficient specimens. The presence of metallic phase is dependent mainly on the temperature and partial pressure of oxygen. Not many workers have reported the appearance of the metallic Zr in samples although their samples also have been sintered in vacuum at $\approx 2000^{\circ}\text{C}$. Annealing in air at about 1000°C results in their rapid reoxidation and transition to white colour and consequent disintegration. The disintegration may be due to either the destructive effects of the Tetragonal \rightleftharpoons Monoclinic transformation temperature or reoxidation of grain boundary metallic phases. Weight changes on reoxidation may also be attributed to either excess oxygen ion vacancy due to sintering in vacuum or reoxidation of the metallic phase.

Thus, keeping the contents of the above report in view, a study of the effect of addition of calcia on the sintering behaviour, stabilization, electrical conductivity, density, mechanical properties and reoxidation behaviour on zirconia sintered in an oxygen deficient atmosphere has been made in the present investigation.

CHAPTER II

SAMPLE PREPARATION

II 1 Raw Materials

The raw materials used for the preparation of samples were as follows

Zirconium oxide from Indian Rare Earth Limited (IRE) and reagent grade calcium carbonate from Sarabhai M Chemicals (with maximum impurity content 1%). The Table II 1 shows the chemical analysis of ZrO_2 as reported by IRE

Table II 1

Chemical analysis of zirconium oxide

ZrO_2 ($ZrO_2 + HfO_2$)	99.5%
Si	0.1%
Fe	0.05%
Ti	0.10%
Al + Mg	0.01%

The amount of ZrO_2 and $CaCO_3$ weighed and mixed for the preparation of the required composition is given in Table II 2 (to make 500 grams of each batch). The batches were weighed and were dry mixed in a centrifugal agate ball mill (Pulverizette, Fritsch, Germany, type 05 102).

Table II 2

Composition	ZrO ₂ mole % (gms)	CaCO ₃ mole % (gms)
C ₀	100 (500)	0
C ₄	96 (490 70)	4 (16 59)
C ₈	92 (481)	8 (34)
C ₁₅	85 (463)	15 (66)

II 2 Precalcination

The batches were heated to 1000°C for 12 hours in a silicon carbide furnace in order to remove CO₂ from CaCO₃

II 3 Presintering

The precalcined batches were dry pressed to make pellets of 2" dia using polyvinyl alcohol as binder. The presintering (calcination) was done in an ASTRO FURNACE MODEL No 1000-2560-FF-20 at 1800°C for 2 hours in a nitrogen gas atmosphere. The samples were heated to 1000°C in 1/2 hr, soaked at 1000°C for 1/2 hr in order to remove the binders and other volatile materials etc and then further heated to 1800°C in 1/2 hr. The samples were soaked at 1800°C for 2 hrs and furnace cooled to room temperature.

II.4 Grinding and Pressing

The pellets were crushed to small pieces and ground in the Agate centrifugal ball mill for 50 hours in distilled

water media. They were dried thoroughly in an oven at 150°C before pressing. 10 cc of 2% polyvinyl alcohol solution and 0.25 gm of paraffin wax in 10 cc of benzene were added as binder and lubricant respectively to every 100 grams of the powder. They were mixed thoroughly by hand, then pressed into rectangular bars and pellets ($\phi = 15$ mm) using high carbon chromium die steel moulds. Pressure was applied slowly till a maximum load of 6 tonnes was attained. The load was held constant for 2 minutes before releasing the pressure in order to homogenise the pressure distribution.

II 5 Sintering

The samples were dried in an oven at 150°C. They were placed in the ASTRO FURNACE with graphite heating elements and fired in a nitrogen gas atmosphere. Temperature was raised to 800°C in 1/2 hr, the samples were soaked at 800°C for 1/2 hr in order to burn off the binder and lubricants. Temperature was raised to 1900°C in 3 hours. The samples were soaked at 1900°C for $1\frac{1}{2}$ hrs and then the temperature was brought down to 800°C in 3 hours before the furnace was shut off. The chemical reaction taking place in the furnace at 1900°C is



From the metal oxide equilibrium diagram, the partial pressure of oxygen at this temperature is found to be $\sim 10^{-11}$ atmosphere [15]

The above samples were used for all further analysis

CHAPTER III

PHASE ANALYSIS

Phase analysis of the samples have been done by two techniques

- 1) X-ray diffraction
- 2) Transmission electron microscopy

III 1 X-Ray Diffraction Technique (XRD)

The concentration of free ZrO_2 in partially stabilized zirconia ceramics is a crucial variable which must be completely controlled. Duwez and Odell [16] have showed that the amounts of phases in these systems can be estimated quantitatively by X-ray diffraction analysis.

X-ray analysis was done on the samples in the as sintered condition and after reoxidation at different temperatures. Several developments have been made on the technique of Duwez et al. [16] and the method adopted to determine the fraction of monoclinic and cubic phases in the present investigation is, the polymorph technique.

III.1 1 Polymorph technique

This technique assumes that the stabilized cubic ZrO_2 phase can be regarded as a high temperature polymorph of ZrO_2 in which integrated intensities are used. Adams and Cox [17] from X-ray intensity calibrations in stabilized and unstabilized ZrO_2 systems showed that

$$I_m(111) + I_m(11\bar{1}) = I_H(111)$$

where I_m is the intensity from the monoclinic phase and I_H is the intensity of the tetragonal or cubic high temperature ZrO_2 polymorph. Therefore, the fraction of monoclinic material in the sample is given by

$$X_m = \frac{I_m(111) + I_m(11\bar{1})}{I_m(111) + I_m(11\bar{1}) + I_c(111)}$$

where I_m and I_c are the intensity from the monoclinic and cubic phase respectively

The standard error of estimate for the values obtained in $CaO-ZrO_2$ system by the polymorph method has been found to be 2.89% [18]

III 1 2 Experimental procedure

X-ray diffraction patterns from all the samples were taken with a RICH SEIFERT ISO-DEBYEFLEX 2002 diffractometer using $CuK\alpha$ ($\lambda = 1.5418 \text{ \AA}$) radiation and nickel filter

Specimens were made by grinding the samples to fine powder and packing them into the circular depression in a perspex holder, the surface was smoothened by passing a plain microscope slide back and forth over it

The X-ray diffraction plots of the samples were measured in 2θ range of 20° to 120° in those compositions which were predominantly cubic and upto 70° in others

The conditions of operation were as given below

Current, voltage	- 30 mA, 40 V
Time constant	- 3 sec
Beam slit width	- 2 mm
Detector slit width	- 0.3 mm
Scan speed	- 3°/min
Chart speed	- 60 mm/min
Full scale intensity	- Between 1000 and 5000 counts/sec

From the diffraction plots of 2θ versus intensity, the diffraction angle θ of each reflection was found and the interplanar spacing 'd' was calculated from the Bragg's relation

$$n\lambda = 2d \sin\theta$$

where n = order of reflection = 1

λ = wavelength of radiation used

d = interplanar spacing

θ = diffraction angle

The calculated 'd' spacings were matched with the standard ASTM datas and the phases were identified [19]

The lattice constant corresponding to each reflection of the cubic phase was calculated from the relation

$$a = d(h^2 + k^2 + l^2)^{1/2}$$

where a = lattice constant

h, k, l = Miller indices of the corresponding reflecting plane.

Precise determinations of unit cell constants of the cubic phase were made by linear extrapolation of the plot of the

lattice constant vs Nelson-Riley-Taylor-Sinclair function for each composition. The function is found by experience [20] to give straight line extrapolation over large ranges of θ . Such a function which has some theoretical justification has been worked out by Nelson and Riley and independently by Taylor and Sinclair. The function is

$$\frac{1}{2} \left(\frac{\cos^2 \theta}{\sin \theta} + \frac{\cos^2 \theta}{\theta} \right)$$

The technique is accurate only when higher angle reflections are considered. The higher angle points only were used for a least square fit.

Integrated intensities were estimated by tracing the peaks on transparent graph sheet and counting the number of squares under each peak.

III 1.3 Results and interpretations

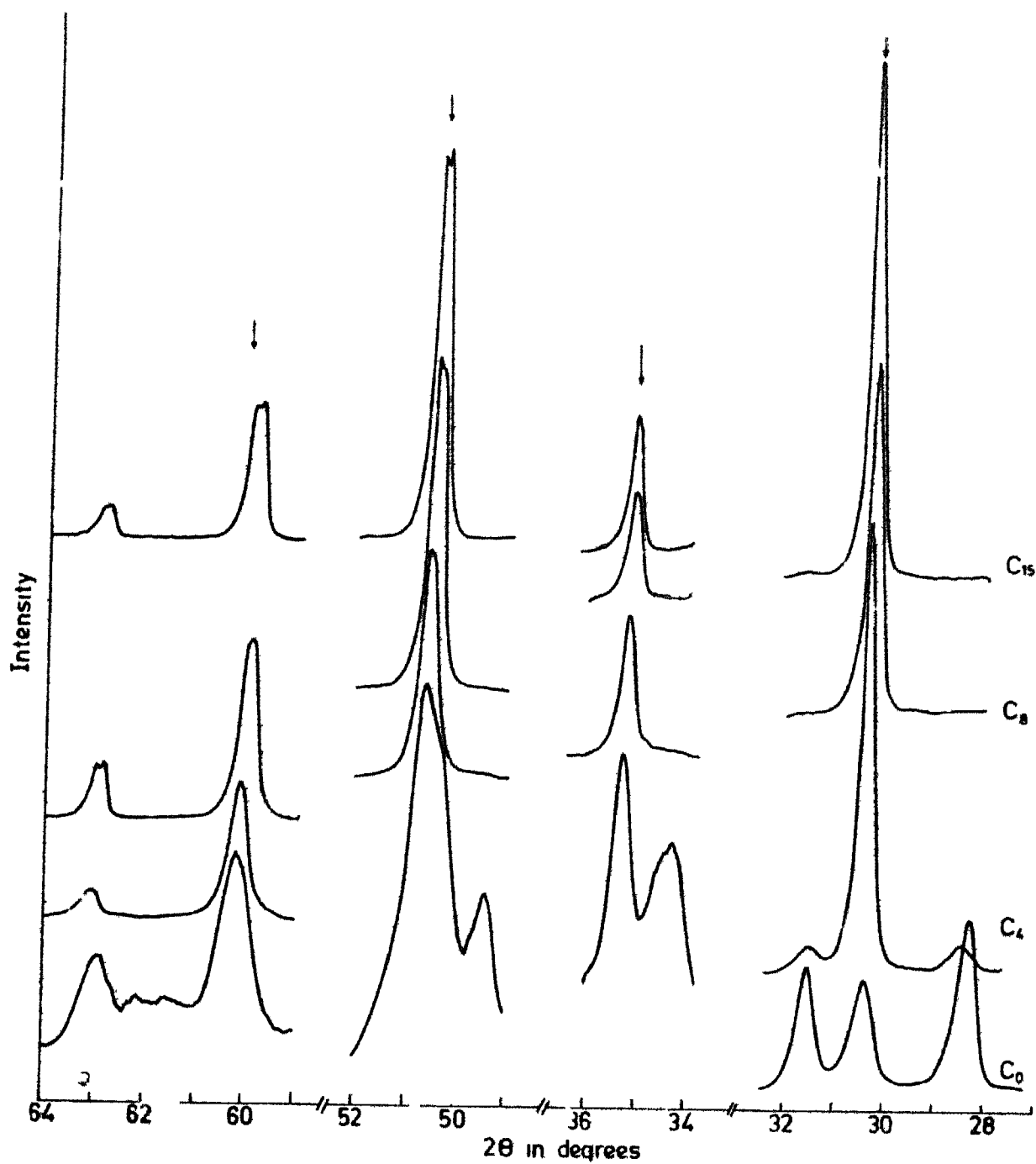
A thin layer of zirconium carbide was found to be present on the surface of the samples, as identified by XRD. This black layer was present only on the surface and could be removed by grinding and polishing and hence no further analysis has been carried out on it in the present study. Carbon for the formation of the zirconium carbide is provided by the graphite heating elements via the gaseous phase as discussed earlier.

The 2 θ values for all the four compositions i.e., C₀, C₄, C₈ and C₁₅ are shown in Table 3.1.1. The 2 θ versus intensity plots in the range 27°-36°, 49°-51° and 59°-64° are shown in Figure 3.1.1.

Table 3 1 1

2 θ values of C₀, C₄, C₈ and C₁₅ compositions

Phase	Plane hkl	ASTM 2 θ	Relative intensity	Observed 2 θ			
				C ₀	C ₄	C ₈	C ₁₅
M	11 $\bar{1}$	28 267	100	28 275	28 425	-	-
C	111	30 192	100	30 375	30 345	30 25	30 225
M	111	31 568	65	31 55	31.6	-	-
M	002	34 263	20	34 3	-	-	-
C	200	35 051	24	35 3	35 1875	35 075	35 05
M	021	38 676	6	38 8	-	-	-
M	21 $\bar{1}$	40 772	14	40 91	-	-	-
M	112	44 987	6	44.98	-	-	-
M	20 $\bar{2}$	45 608	8	45 575	-	-	-
M	022	49 395	18	49 39	-	-	-
C	220	50 416	80	-	50 575	50 4	50 3
M	11 $\bar{2}$	50.686	12	50 6	-	50 475 }	50.4 }
M	130	56 076	8	56.0	-	-	-
M	31 $\bar{1}$ 212	57 294	8	57.25	-	-	-
C	311	60 077	60	60 2	60.125	59 95 60.05 }	59.8 59.925 }
M	21 $\bar{3}$	62.082	10	-	-	-	-
C	222	62 782	10	-	63 05	62.85 63 0 }	62.725 62.85 }
M	311	62.972	6	-	-	-	-
M	321 320	65 760	6	-	-	-	-
C	400	74 064	12	-	74 30	74.1	73.925
C	331	82 43	20	-	82 175 82 325 }	82.06 82 2 }	74.075 81.8375 }
C	420	84.53	-	-	84 9	84 6 84.8 }	84.425 84.65 }
C	422	95 676	16	-	95 25 95.45 }	95.05 95 3 }	91.7875 95.05 }
C	333	103 743	14	-	103 15 103 4 }	102 9 103 2 }	102.625 102.975 }
C	440	117 864	5	-	-	116 7 117.15 }	-



3 1 1

X-ray diffraction patterns for different compositions. Arrows indicate ASTM cubic ZrO_2 peak positions.

There is a considerable amount of variation in the amount of cubic phase as the calcia content varies in the samples. From Table 3 1 2 it is seen that the C_0 sample (with no CaO addition) contains 30% cubic phase, fraction of the cubic phase increases with the CaO content and the 8/ and 15% CaO samples are fully cubic.

Sintering in an oxygen deficient atmosphere is known to reduce the temperature at which the tetragonal-cubic transformation takes place. Ruh and Garrett [21] found that this temperature drops from above $2240^\circ C$ to about $1490^\circ C$ as the oxygen content in zirconia reduces from 66.6 a/o to 63 a/o. However no cubic phase is expected to be present at room temperature even when the oxygen content is as low as 55 a/o according to the phase diagram for oxygen deficient zirconia proposed by Ruh and Garrett. Instead a mixture of tetragonal zirconia and metallic zirconium is expected below 65 a/o oxygen content. However their data was obtained by equilibrating mixtures of zirconium metal at 10^{-5} torr and the results may not be strictly comparable with the present results.

The stabilization of the cubic fluorite structure at zero or low calcia content can be explained on the basis of nonstoichiometry in the lattice due to sintering in the highly reducing atmosphere at extremely low partial pressure of oxygen, 10^{-11} atmosphere. At these low partial pressures of oxygen, a large number of O^{2-} vacancies are expected to be created, an effect also produced by the addition of stabilizers such as CaO . Thus sintering in oxygen deficient

Table 3 1 2

Percentage and lattice constants of the as sintered and reoxidized samples (cubic phase)

	C_0	C_4	C_E	C_{15}
/ cubic phase (as sintered)	30	85	100	100
Lattice constant	5 087 Å	5 109 Å	5 116 Å	5.127 Å

% cubic phase (reoxidized 1000 C)	4	25	91 38	92.5

% cubic phase (reoxidized 1350°C)	11 11	41 30	92 5	95 6
Lattice constant	-	5 113 Å	5 120 Å	5 132 Å

atmosphere has a stabilising effect similar to that due to CaO

The 2θ values of the cubic peaks of C_0 and C_4 are high when compared to the ASTM standard data [19]. Although their values are closer to the tetragonal peaks, they are confirmed to be cubic peaks on the basis of following two reasons

- Absence of 20%, 40% and 40% intensity reflections at $2\theta = 34.646^\circ$, 59.608° and 73.330° respectively
- On reoxidation of the sintered samples in air, there is a marked decrease in the 2θ values which come closer to the ASTM standard values of cubic reflections.

The Nelson-Riley plot showing the determination of accurate lattice constant by extrapolation method is shown

in Figure 3 1 2 and Table 3 1 3. The high angle points have been fitted to a straight line by a least square method. Due to nonavailability of distinct peaks at higher angles, the Nelson-Riley plot could not be drawn for C_0 . Considering the marked increase in the 2θ values of the 100% and 24% intensity peak, it can definitely be assumed that there is a shrinkage in the lattice.

Figure 3 1 3 shows the variation of lattice constant with composition. It is seen that lattice constants of $C_{15} > C_8 > C_4 > C_0$. Considerable amount of contraction of the lattice of C_0 and C_4 with respect to ASTM standard values has been observed. The samples were reoxidized in air at 1000°C for 12 hours and 1350°C for 15 hours. Nelson-Riley plots (Figure 3 1 4) were drawn for the precise determination of the lattice constants of the cubic phase for the specimens oxidized at 1350°C. The variation of lattice parameter of the samples in as sintered conditions and on reoxidation are shown in Figure 3 1 3 and Table 3 1 2. There is an increase in the lattice constant values on reoxidation. This clearly shows the effect of oxygen deficiency due to sintering in oxygen deficient atmosphere.

The percentage of cubic phase has been plotted as a function of reoxidation conditions in Figure 3 1 5 and tabulated in Table 3 1 2. It is observed from them that all compositions contain cubic phase and destabilization occurs on reoxidation at both 1000°C and 1350°C. It is interesting to note that the relative amount of cubic phase retained on heat treatment at 1350°C/15 hours is more as compared to the

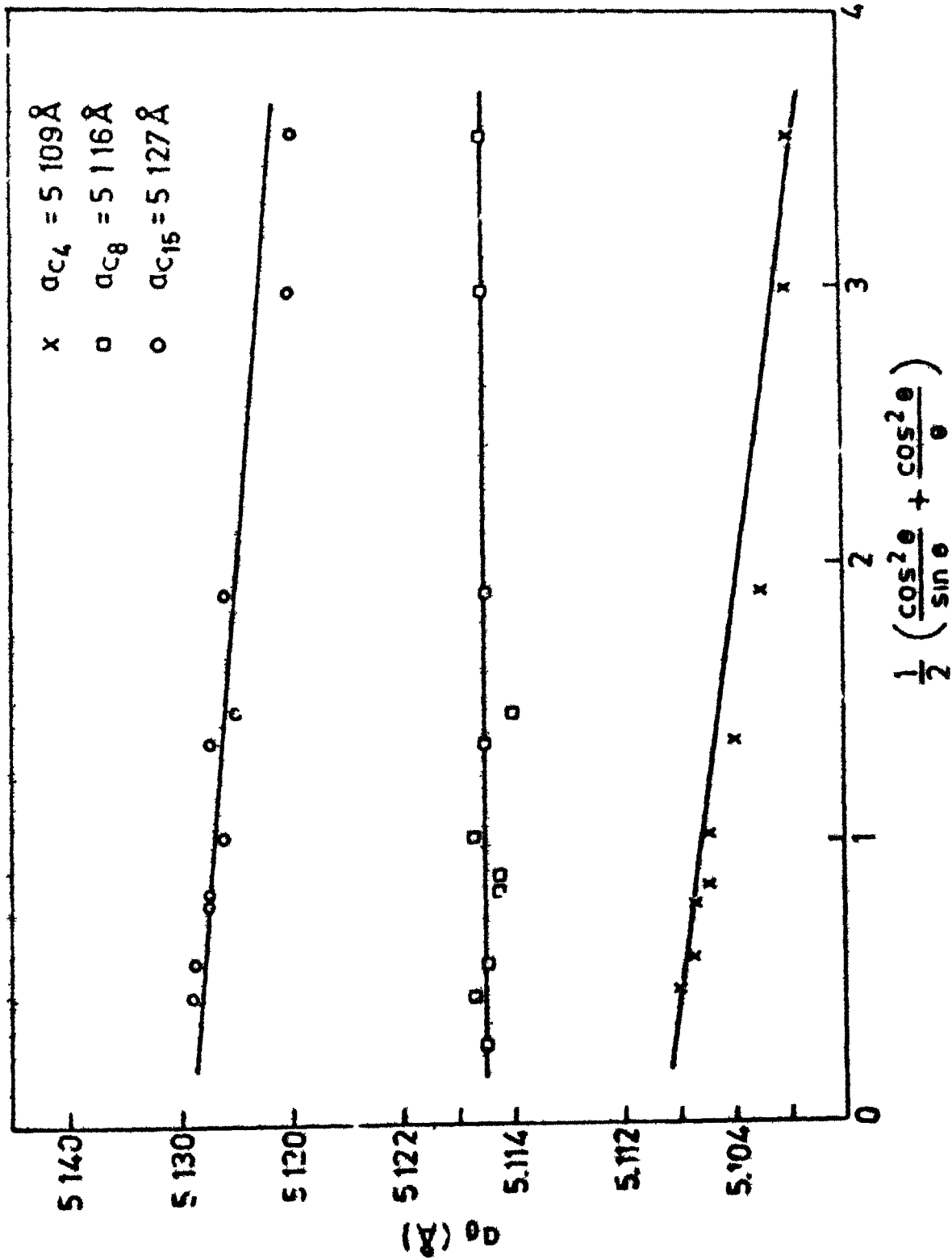
Table 3 1.3
Lattice parameter of cubic phase

Composition	2θ	hkl	d (Å)	a (Å)	Extrapolated a (Å)
C ₀	30 375	111	2 942	5 090	5 087
	35 3	200	2 542	5.084	
C ₄	30 345	111	2 944	5 100	5 109
	35 1875	200	2 550	5 100	
	50 575	220	1 804	5 102	
	60.125	311	1 538	5.100	
	63 05	222	1 474	5.106	
	74 30	400	1.276	5 106	
	82 175	331	1 171	5 106	
	82 325		1 172		
	84 9	420	1 142	5.107	
	95 25	422	1.042	5 107	
	95 45		1.042		
	103 15	333	0 983	5.108	
	103 4		0 983		
C ₈	30.25	111	2.954	5 116	5 116
	35 075	200	2.558	5 116	
	50.4	220	1.809	5.116	
	50 475		1 809		
	59 95	311	1.542	5 114	
	60 05		1 542		
	62 85	222	1 477	5 116	
	63 0		1.476		
	74.1	400	1 279	5 117	
	82.05	331	1 173	5 115	
	82 2		1 173		
	84 6	420	1.144	5 118	
	84 8		1.144		
	95.05	422	1.044	5.116	
	95.3		1.044		
	102 9	333	0.984	5.117	
	103 2		0.984		

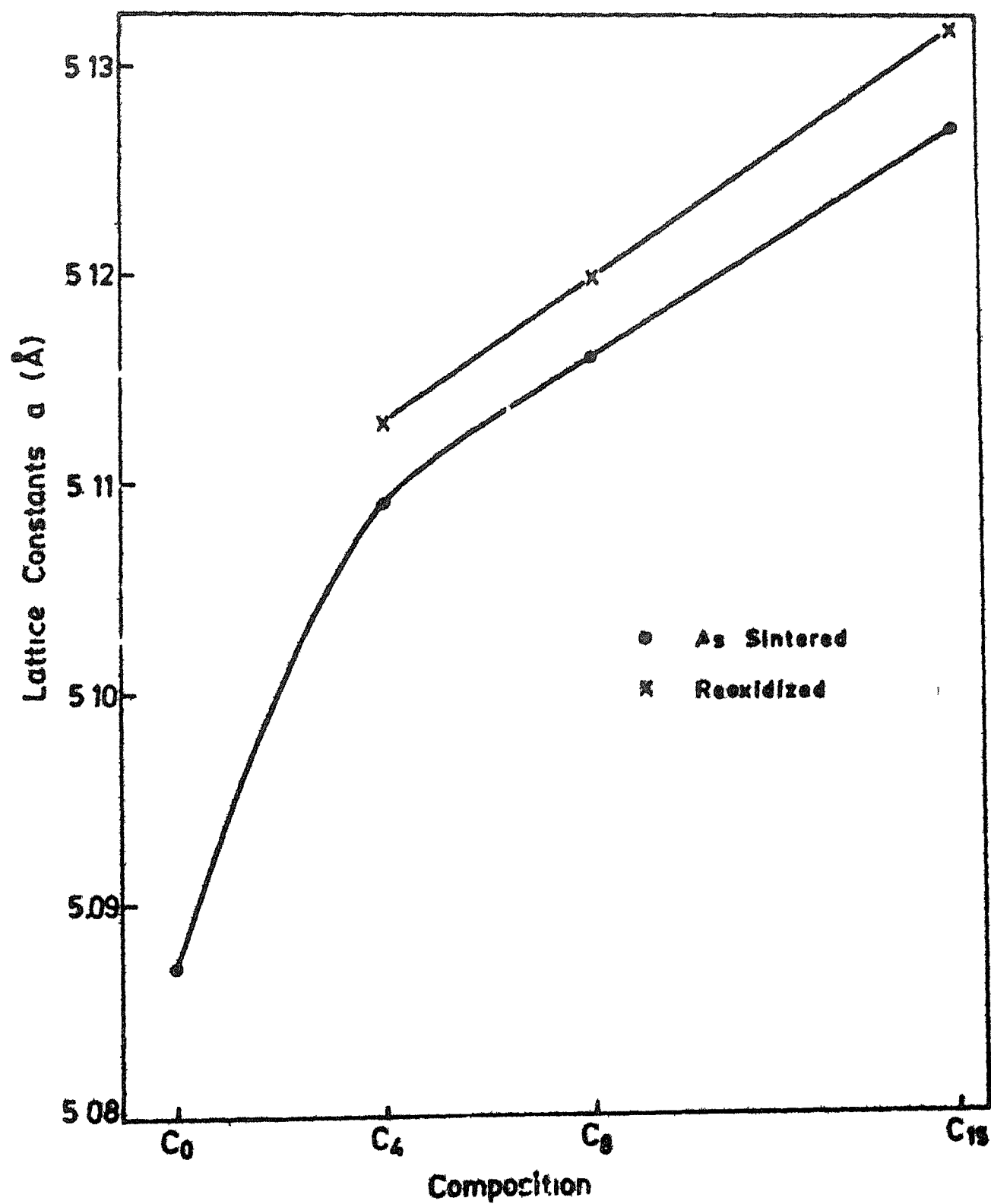
Contd...

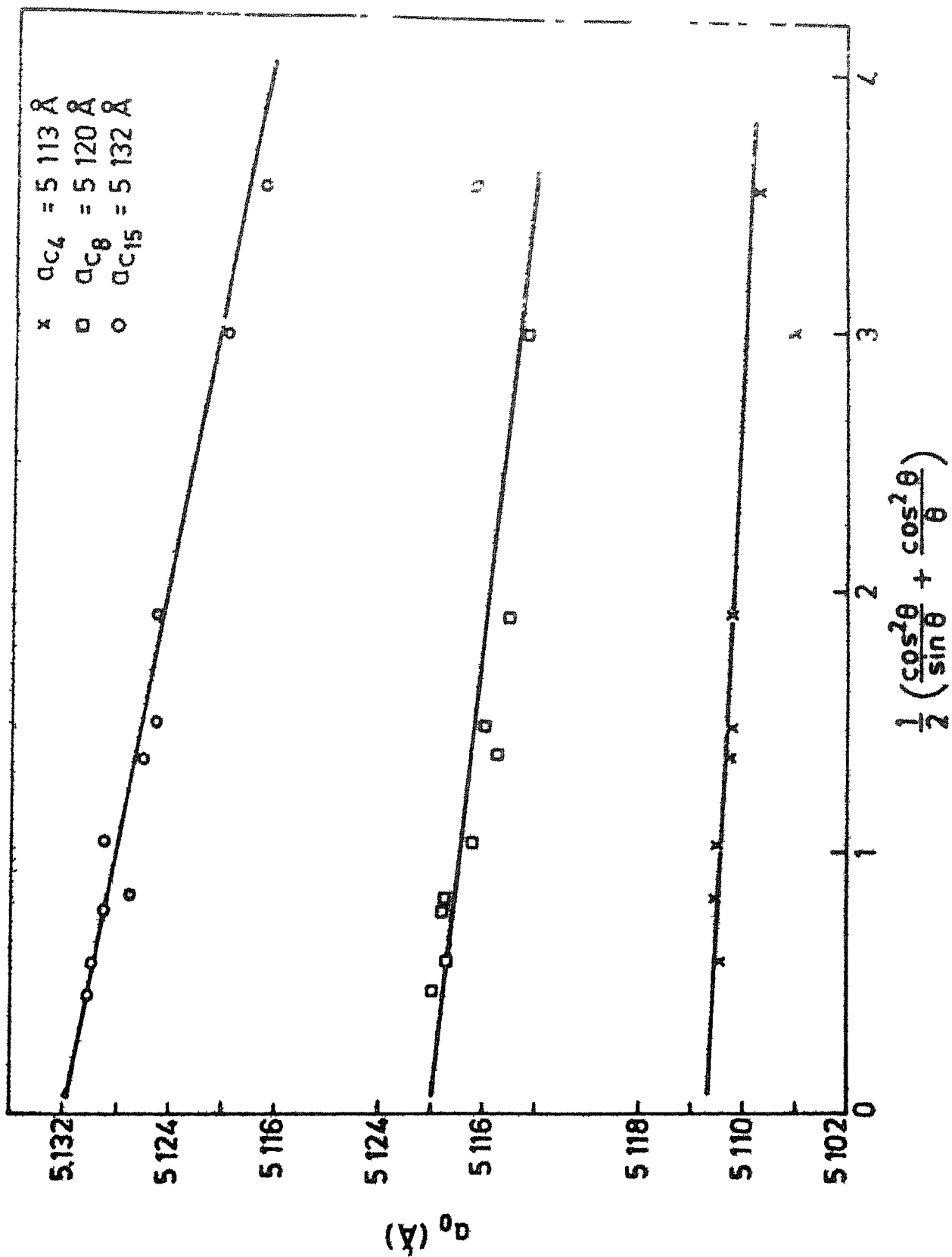
Table 3 1.3 (continued)

Composition	2 θ	hkl	d (Å)	a (Å)	Extrapolated a (Å)
C ₈	116.7	440	0.904	5.115	5.127
	117.15		0.904		
C ₁₅	30.225	111	2.959	5.120	
	35.05	200	2.56	5.120	
	50.3	220	1.812	5.125	
	50.4		1.812		
	59.8	311	1.545	5.124	
	59.925		1.545		
	62.725	222	1.48	5.126	
	62.85		1.48		
	73.925	400	1.28	5.725	
	74.075		1.28		
	81.8375	331	1.176	5.126	
	82.05		1.175	5.122	
	84.425	420	1.146	5.126	
	84.65		1.146		
	94.7875	422	1.046	5.127	
95.05	1.046				
102.625	333	0.986	5.127		
102.975		0.986			

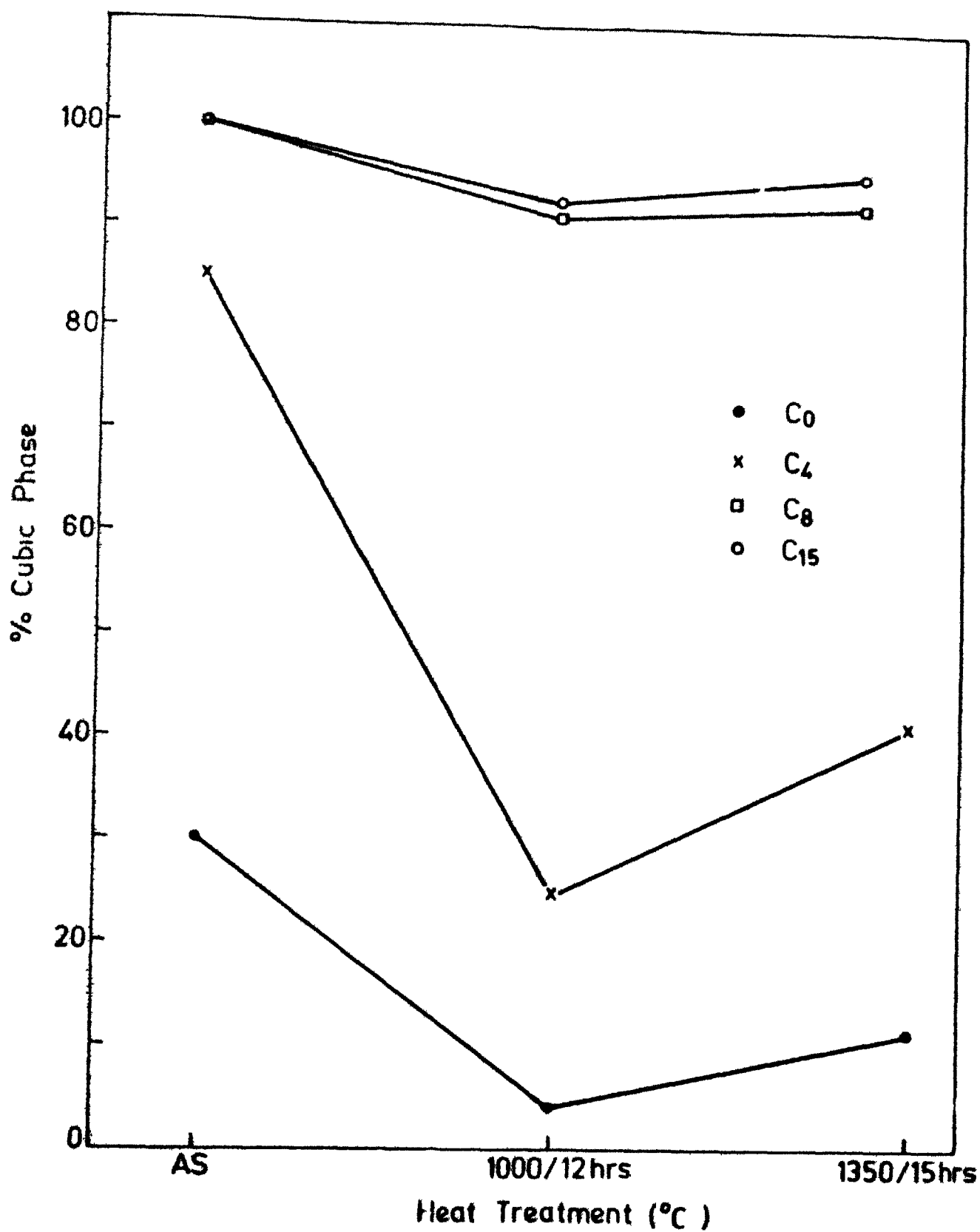


3 1 2 Nelson-Riley plots for determination of lattice constants of different compositions in as sintered condition





3.1 4 Nelson-Riley plots for determination of lattice constants of different composition in reoxi-



amount on heat treatment at 1000°C/12 hours. This shows that destabilization is more easy around the Tetragonal \rightleftharpoons Monoclinic transformation temperature.

The phase analysis by X-ray diffraction thus indicates that sintering in oxygen deficient atmosphere causes anion vacancies to form and thereby has a stabilizing effect. There is an overall increase in the volume of the lattice on reoxidation. The destabilization effect is relatively more easy on reoxidation at 1000°C.

III 2 Transmission Electron Microscopy

It has been reported by Carniglia and co-workers [11] that the O deficiency in ZrO_2 is limited by the appearance of a metal phase which was always observed on vacuum sintering at 2100°C under 1.3×10^{-7} atmospheric pressure.

In order to analyse the presence of any metallic phase if present, phase analysis was also done by transmission electron microscopy. Selected area diffraction mode was adopted for obtaining diffraction patterns.

III 2 1 Experimental procedure

Diffraction patterns were obtained by using a PHILIPS TRANSMISSION ELECTRON MICROSCOPE MODEL 301. The operating conditions were as follows:

- 1) Goniometer stage fitted
- 2) Voltage used - 100 KV

The samples were analysed in the powder form. They were ground to as fine a powder as possible. A thin film

of carbon was placed on a copper grid and a drop of the suspension of the powdered sample in acetone was placed on it

In order to make precise measurements of the camera constant, each time an experiment was conducted, the diffraction pattern of standard gold sample was taken in the same conditions in which the diffraction pattern of specimen was taken. The diffraction pattern of a standard specimen of gold and the plot of R versus $(h^2 + k^2 + l^2)^{1/2}$, where R is the radius of the rings of the diffraction pattern and h, k, l are the miller indices of the corresponding planes is given in Figure 3.2.1. The camera constant $L\lambda$ was calculated from the relation

$$Rd = L\lambda \quad (1)$$

The slope of the plot of R versus $(h^2 + k^2 + l^2)^{1/2}$ multiplied with the lattice constant of gold ($= 4.0788 \text{ \AA}$) gave the camera constant.

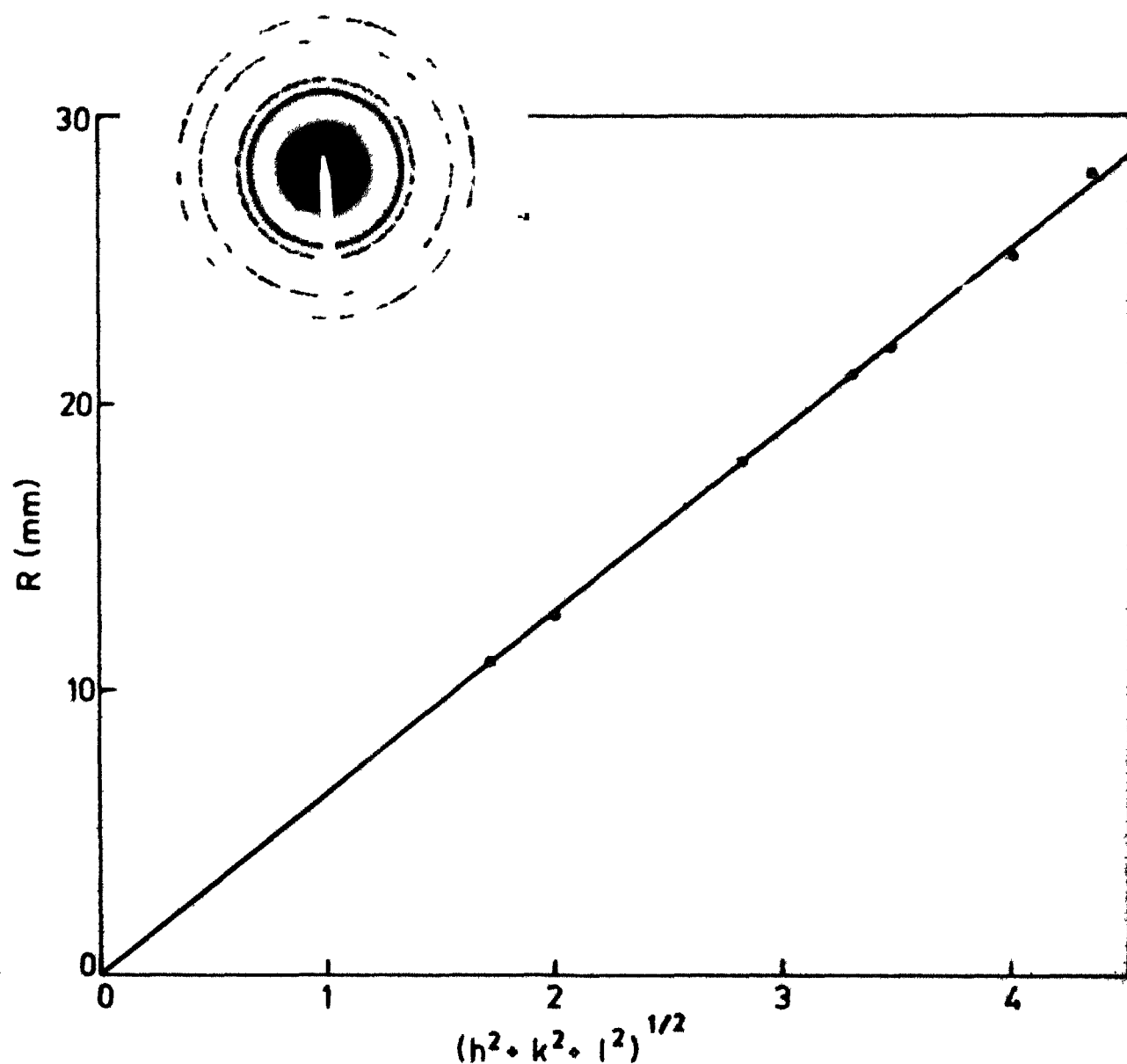
The diffraction patterns of the as sintered samples were indexed in the following manner

Three spots close to the transmitted beam were chosen. Their distances R from the transmitted beam spot and also the angle between the spots were measured.

From the relation (1)

$$d = \frac{L\lambda}{R}$$

' d ' values were computed for the three spots knowing $L\lambda$ and R . They were matched with the ' d ' values of the ASTM.



3 2 1

Variation of R with $(h^2 + k^2 + l^2)^{1/2}$ for a diffraction pattern of gold

standards of a particular composition Particular attention was given to detection of Zr metal, and hence, the calculated 'd' values were matched with ASTM standards of zirconium metal and secondly with that of cubic ZrO_2 and m- ZrO_2 If the three d values matched with any of the three planes given in the ASTM standard for a particular composition, the angles between the corresponding planes were calculated, keeping the structure of the material in mind

Let ϕ be the angle between two planes or miller indices $(h_1 \ k_1 \ l_1)$ and $(h_2 \ k_2 \ l_2)$

In the cubic system

$$\cos\phi = \frac{h_1 h_2 + k_1 k_2 + l_1 l_2}{(h_1^2 + k_1^2 + l_1^2)(h_2^2 + k_2^2 + l_2^2)^{1/2}}$$

In the hexagonal close packed system

$$\cos\phi = \frac{h_1 h_2 + k_1 k_2 + \frac{1}{2}(h_1 k_2 + h_2 k_1) + \frac{3}{4} \frac{a^2}{c^2} l_1 l_2}{(h_1^2 + k_1^2 + h_1 k_1 + \frac{3}{4} \frac{a^2}{c^2} l_1^2)(h_2^2 + k_2^2 + h_2 k_2 + \frac{3}{4} \frac{a^2}{c^2} l_2^2)^{1/2}}$$

where a and c are the lattice constants

If the measured angle matches with the calculated angle within an experimental error of 5% it can confirmatively be concluded that the pattern has been indexed correctly which indirectly confirms the presence of the composition of our interest in the specimen

The beam direction was found from the cross product of those two indexed spots which have the lower angle between them.

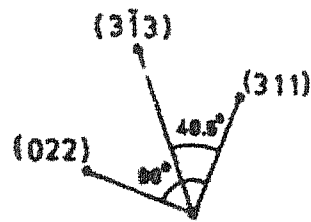
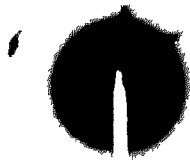
III 2 3 Results and interpretation

The diffraction patterns of all the four compositions C_0 , C_4 , C_8 and C_{15} were analysed. The diffraction patterns of as sintered samples of C_8 and C_{15} are shown in Figures 3 2 2 and 3 2 3 respectively.

Apart from the cubic and monoclinic phases in the as sintered samples of C_0 and C_4 , and the cubic phase in C_8 and C_{15} a minor amount of third phase was also present in C_8 and C_{15} samples. Selected area diffraction identified this phase as metallic zirconium. As the XRD analysis did not show any metallic zirconium peaks, the amount of metallic zirconium in C_8 and C_{15} must be less than 5%, the lower limit of detection of a phase by X-rays. This implies that the composition C_8 and C_{15} are so oxygen deficient that they contain free Zr in the lattice although this much reduction is not obtained when either C_0 or C_4 are fired at this temperature. This indicates that formation of Zr metal is not the result of only nonstoichiometry due to sintering at 1900°C in an oxygen deficient atmosphere but is also aided by the formation of oxygen ion vacancies caused by the replacement of Zr^{4+} by Ca^{2+} to maintain charge neutrality, on addition of enough amount of calcia.

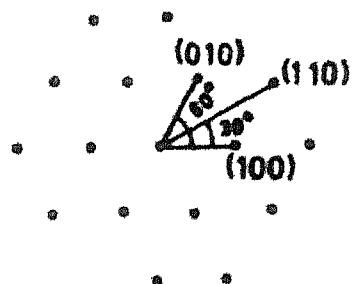
All the diffraction patterns were taken from the edge of the particle (sample) since the sample thickness in the mid portion made it impossible to give identifiable patterns. Hence it could not be confirmed if Zr metal is present as a grain boundary phase or if it is present in the

Composition Cb



CUBIC ZrO_2

$d(\text{\AA})$	hkl	\vec{B}
1.575	311	$[2\bar{3}\bar{3}]$
1.7655	$0\bar{2}2$	
1.19	$3\bar{1}3$	



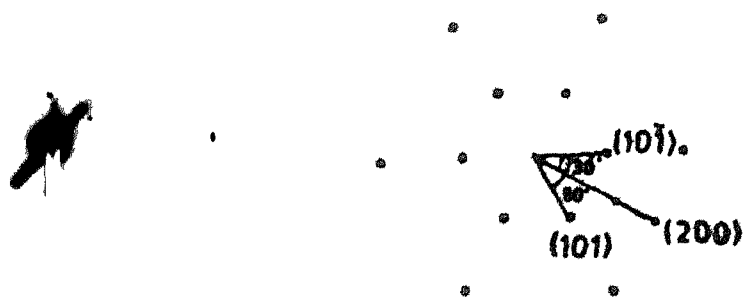
Zr Metal

$d(\text{\AA})$	hkl	\vec{B}
2.69	100	
2.69	010	$[001]$
1.55	110	

3 2 2

Diffraction patterns of as sintered samples of Cg indicating presence of cubic ZrO_2 and metallic Zr

Composition C₁₅



Zr Metal

$d(\text{\AA})$	hkl	\vec{B}
2.51	101	
2.51	$10\bar{1}$	$[020]$
1.456	200	

3 2 3 Diffraction patterns of as sintered samples of
C₁₅ indicating presence of Zr metal

form of discrete particles within the compact. However as seen in a later chapter, the microstructure analysis by scanning electron microscope (SEM) shows Zr metal phase to be present in discrete particles within the compact, their concentration being more towards the edge of the specimen.

CHAPTER IV

MICROSTRUCTURE ANALYSIS

X-ray analysis and electron microscopy showed the presence of the following phases in the as sintered specimens

- a) A thin layer of zirconium carbide on the surface of each specimen.
- b) Both monoclinic and cubic phase in C_0 and C_4 and cubic phase and metallic Zr in C_8 and C_{15}

In order to analyse the exact distribution of the phases, microstructure analysis was performed by scanning electron microscopy

IV 1 Experimental Procedure

An ISI-60 scanning electron microscope was used to analyse the specimens. Cross sections of the specimens were ground to a thickness of ≈ 3 mm and thereafter polished on a glass plate with 100, 240, 400, 600 and 800 grit size silicon carbide powder. They were finally polished with 0.5 μ size alumina powder in a polishing wheel. The final thickness of the specimens used for microstructure analysis was less than 1 mm. Since evidence for the presence of zirconium metal in some compositions was obtained as discussed in the earlier chapter, the samples were not etched because etching could result in the removal of the metallic phase.

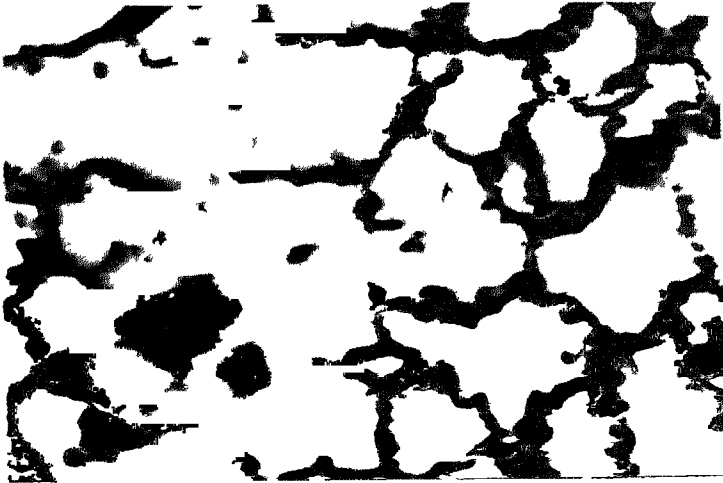
The specimens were mounted on aluminium sample holder with silver paint. A thin layer of gold was coated on the surface of the specimen by sputtering.

IV 2 Results and Interpretation

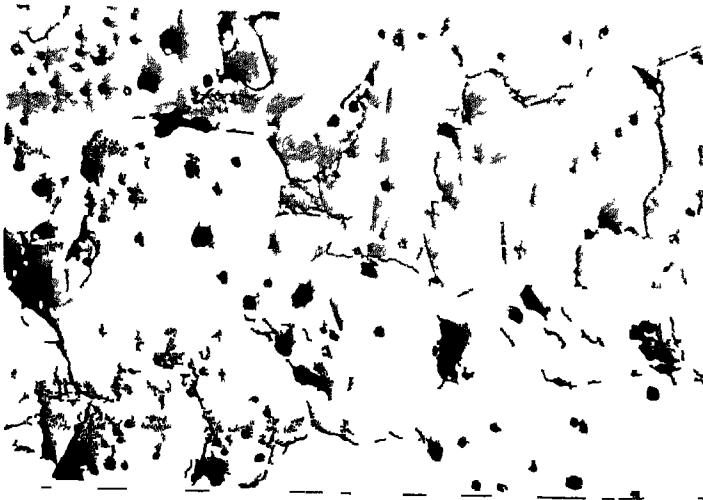
The microstructure of the four compositions C_0 , C_4 , C_8 and C_{15} were studied.

As mentioned earlier a thin layer of zirconium carbide was found to be present on the surface of all specimens. Figure 4.1 shows the secondary electron image of the edge of a C_0 specimen. It consists of randomly shaped bright grains surrounded by a dark and thick continuous phase. The dark phase surrounding the grains is present only near the edge of the specimen. Figure 4.2 shows the back scattered electron image of the mid portion of the C_0 specimen. It is seen very clearly that there is no second phase surrounding the grains. X-ray analysis (Section III.1) has shown that zirconium carbide is formed during sintering only near the surface of the specimen. It is believed that the dark grain boundary phase in Figure 4.1 is zirconium carbide. The bright grains are the monoclinic and cubic zirconia which however could not be identified individually.

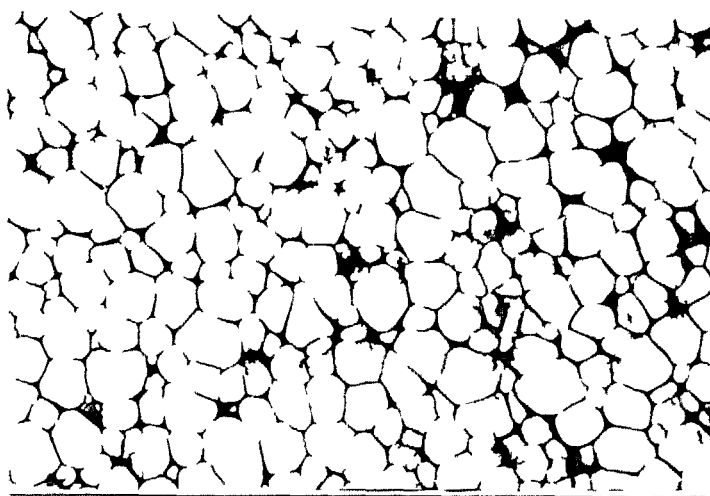
Figures 4.3 to 4.9 show the back scattered image of C_4 , secondary and back scattered images of mid portion of C_8 , secondary and back scattered images of central portion of C_{15} and finally the back scattered images of the edge of C_8 and C_{15} specimen respectively.



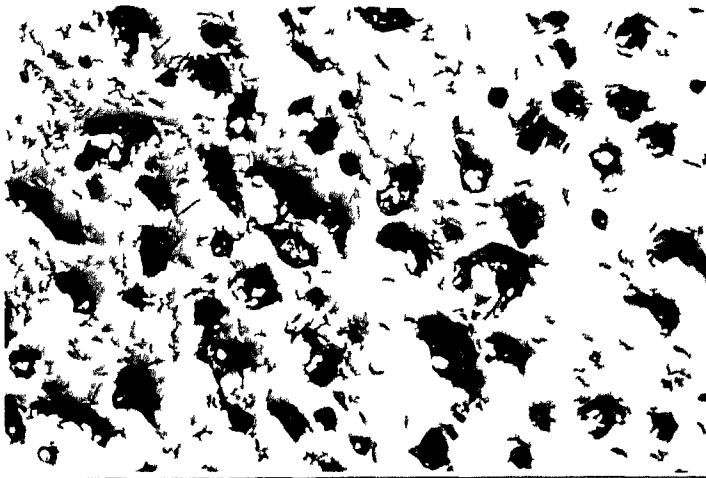
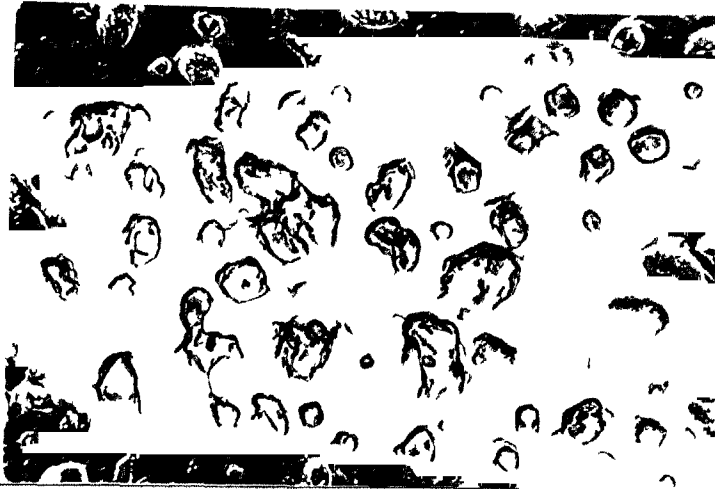
4.1 Secondary electron image of the edge of a C₀ sample (200x)



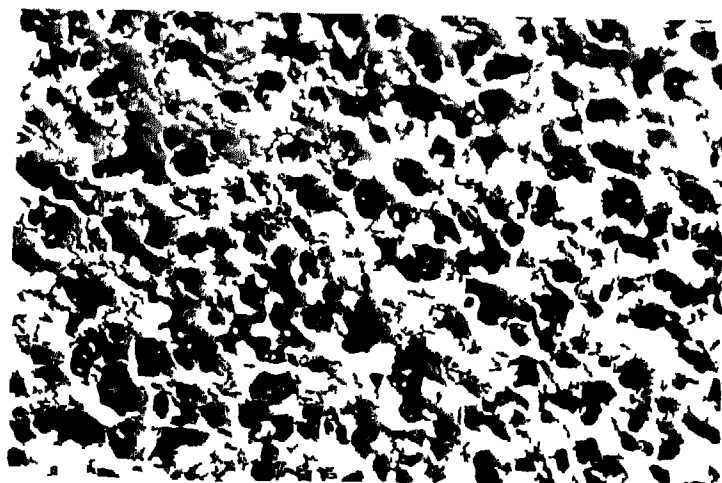
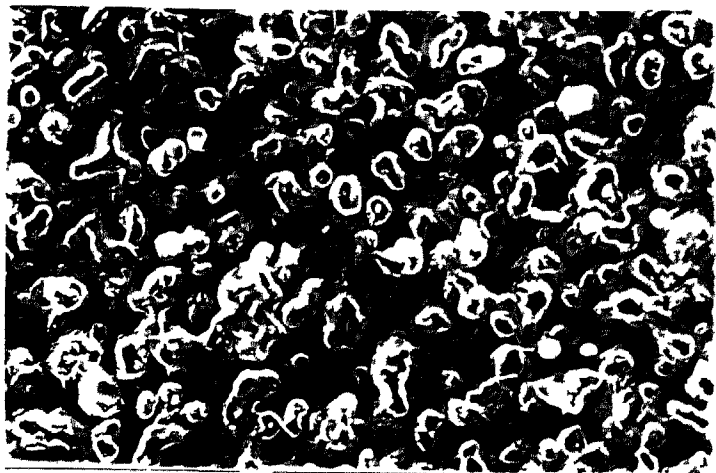
4.2 Back scattered electron image of the mid portion of C₀ specimen (200x)



4 3 Back scattered electron image of C₄ sample
(200x)



4 4 & Secondary electron and
4 5 back scattered electron images of the same region
(mid portion) of C₈ sample (200x)
While patches in the pores (Figure 4 5) indicate
Zr metal



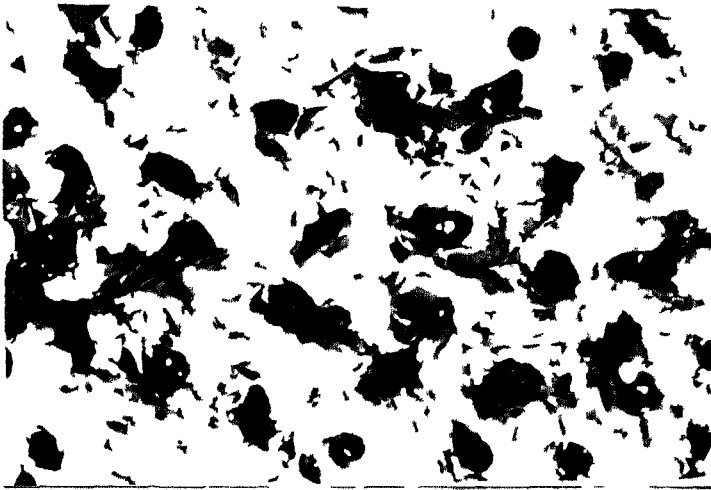
4.6 &
4 7

Secondary electron and
back scattered electron images of the same
region (mid portion) of C₁₅ sample (200x)



4 8

Back scattered electron image of edge of C₈
sample (480x)



4 9

Back scattered electron image of edge of C₁₅
sample (400x)

On comparing the microstructure of all the four compositions it is seen very clearly that the shape and size of the grains of C_4 are entirely different from the rest of the compositions. The size of the grains are relatively small, appear smooth and rounded unlike the grains of C_0 , C_8 and C_{15} . This might be the result of less oxygen deficiency in the specimen due to an error caused inadvertently during the sintering of C_4 samples.

The grain boundaries of the C_8 and C_{15} specimens were not distinct since the samples were not etched. The microstructure in SE image (Figure 4.4) consists of a continuous phase which would be cubic zirconia and dark region which are pores. The BSE image of the same region (Figure 4.5) shows small white region within the pores which are believed to be discrete particles of metallic zirconium. The phase having maximum concentration of the high atomic number element (Zr) is expected to be brightest in the back scattered image. The appearance of zirconium metal in the form of discrete particles can be explained on the basis of high value of dihedral angle as reported by Virkar and Lynn Johnson [22]. They found the dihedral angle between Zr metal and ZrO_2 to be 88° . This results in the Zr metal not wetting the surface of the zirconia grains; the metal tends to reach the outer flat surface of the specimen after long annealing treatment to minimize the energy.

If sufficient time for migration of the metal to the surface is not available the metal would tend to stay at the next energetically favourable site which are the

free surface provided by the pores. This is what is observed by us. The metal has tended to form into spheres so as to minimum contact with the zirconia surface.

It is observed that the concentration of zirconium metal, both in C_8 and C_{15} is relatively higher at the edges when compared to the middle portion of the same specimens. This is seen clearly in Figures 4.8 and 4.9 respectively. The reason is because the oxygen ions are removed by diffusing to the surface of the specimens, the diffusion distance for the central region being large, that region is less deficient in oxygen and poorer in metallic zirconium than the region near the surface.

It is also observed on comparison of the microstructures of C_8 and C_{15} specimens, the amount of zirconium present in the C_8 specimen is relatively more than that of C_{15} . The reason for this is not very clear and could be due to limited number of observations. Further experiments have to be conducted to explain this behaviour.

Thus the important observation from SEM is the presence of zirconium metal at the pores between the grains. This observation is supported by the following

- (1) Transmission electron microscopy observations.
- (2) Concentration of Zr metal more at the edges; had it been an artefact the concentrations would have been uniform throughout the sample.
- (3) Absence of features corresponding to metallic Zr in specimens of C_0 and C_4 . TEM also did not show any metallic phase in the specimens of C_0 and C_4 .

Thus it is confirmed that specimens of C_0 and C_4 do not contain any metallic zirconium phase and specimens of C_8 and C_{15} contain metallic zirconium in the form of discrete particles, concentrated at the pores

CHAPTER V

CONDUCTIVITY MEASUREMENTS

Fully CaO stabilized zirconia $Zr_{0.85}Ca_{0.15}O_{1.85}$ has been shown to be a suitable electrolyte for the determination of oxygen potential in oxide systems. It is generally accepted that the conductivity of zirconia stabilised in the fluorite structure by additions of divalent and trivalent oxides is essentially ionic over a wide range of temperature and that the mobile ions are the anions.

Electrical conductivity measurements by Hund, Trombe and Foex, Kingery et al. [23] and other workers have revealed rather high electrical conductivities for the cubic solid solutions in the system ZrO_2 -CaO at elevated temperatures. Tien and Subba Rao [23] report that anion vacancy is fixed by composition i.e. each molecule of CaO added introduces one anion vacancy due to replacement of Zr^{4+} by Ca^{2+} . Contrary to the expectation that conductivity increases with increase in defect concentration actual data show that maximum conductivity occurs at the lower limit of single phase cubic region which is about 12-13 mole % calcia for ZrO_2 -CaO solid solution. Tien and Subba Rao proposed the following model to explain this behaviour.

The oxygen ion which is the charge carrier has to pass between two types of metal ions to reach an anion site which may be one Zr^{4+} and Ca^{2+} each, $2Ca^{2+}$ or $2Zr^{4+}$. The energy required for an oxygen ion to pass between two

Ca^{2+} is largest since Ca^{2+} is 25% larger than Zr^{4+} . The probability of this occurring increases with increase in calcia content. Hence the activation energy increases and consequently the conductivity decreases at a given temperature with increase in calcia content. Between the calcia content of 0 to 12 mole % in ZrO_2 , the microstructure consists of both cubic and monoclinic phases. The conductivity of the monoclinic phase is less than that of the cubic phase. As the calcia content increases in this range, the conductivity also increases.

Below 650°C , the contribution to conductivity in C-ZrO_2 is mainly due to diffusion through the grain boundaries while at the higher temperature the conductivity is predominantly due to grain

Hence the conductivity of a sample of zirconia will depend on the relative amount of the phases present and on the microstructure. In addition other effects may be expected in samples which have been sintered in highly oxygen deficient atmosphere because of the presence of additional anion vacancies.

V 1 Experimental Procedure

A 1608 impedance bridge manufactured by General Radio was used to conduct the tests. A EUROTHERM temperature controller with a precision of 1°C was used to control the temperature. A C conductivity with an alternating voltage applied across the samples was measured at a frequency of 1 KHz.

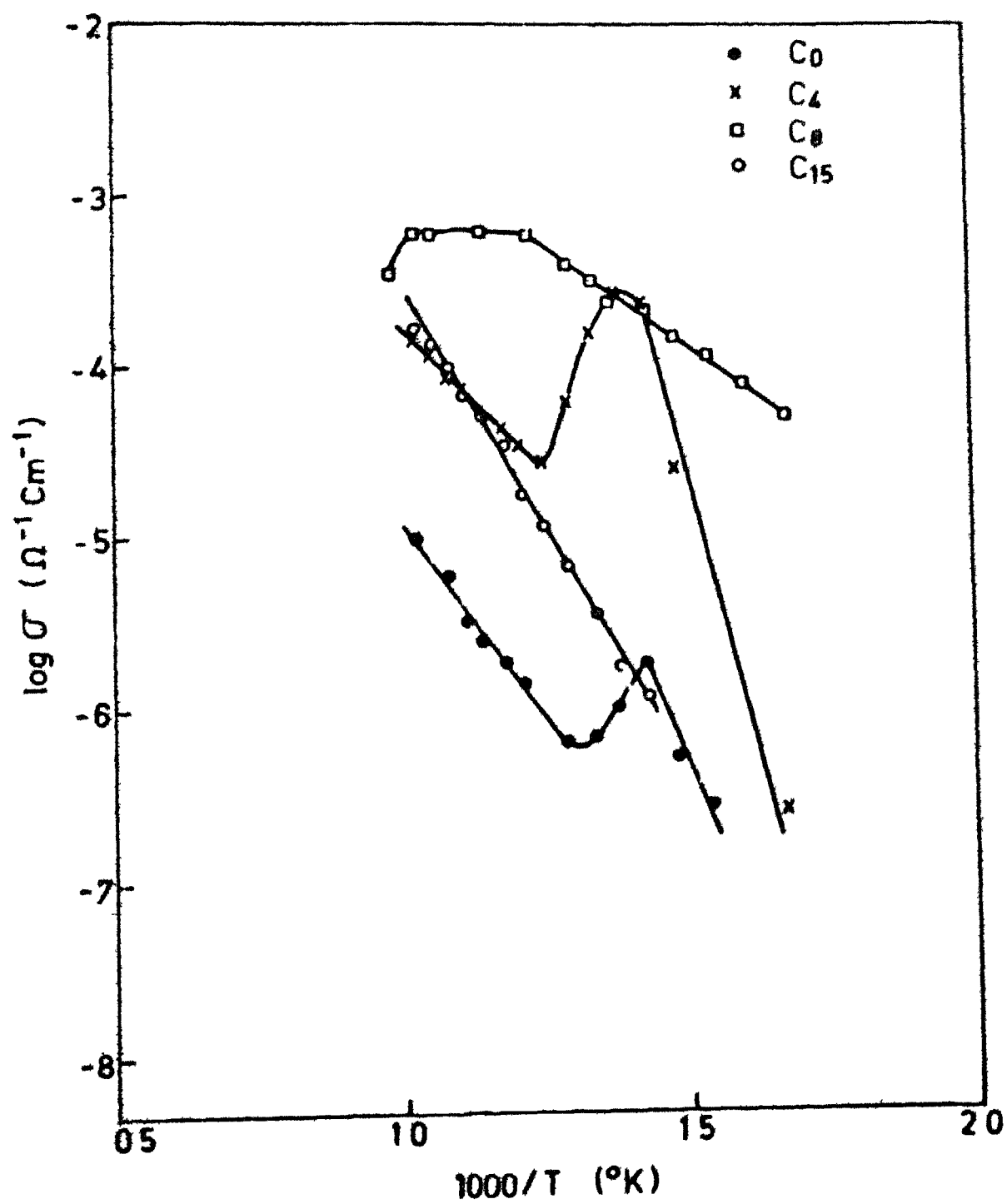
The electrodes were made of platinum which were fused with silver lead wires. They were held in position between two ceramic supports. Platinum foils were placed on the electrodes to avoid their contamination by samples. Pressure was applied by the compression of spring placed between two ceramic supports. The lead wires were enclosed in a teflon cylinder to avoid any contact among themselves and with the thermocouple used for the measurement of temperature.

About 20 minutes were given at a particular temperature for the sample to attain thermal equilibrium.

V.2 Results and Interpretation

The $\log \sigma$ versus $\frac{1}{T}$ plot is shown in Figure 5.1. It is seen that between 250°C and 400°C and also between 450°C and 700°C the conductivity increases with increase in amount of calcia added till the composition C_8 is reached i.e. $\sigma_{C_8} > \sigma_{C_4} > \sigma_{C_0}$ and drops on further addition of calcia as seen by a fall in C_{15} . This result is in agreement with that of Tien and Subba Rao [23].

A remarkable feature is observed in the same plot. The conductivity for C_0 , C_4 and C_8 compositions increases with increase in temperature, reaches a maximum and then drops before rising again with further increase in temperature. It is observed that the temperature at which the peak occurs, increases with increase in calcia content. Thus it is possible that the same trend would be observed in the case of C_{15} also at a temperature above 700°C, if



the experiments could be carried out to higher temperatures. It is interesting to note that the width of the peak increases with increase in calcia content. Although it is difficult to comment on the observed peaks in the conductivity without some additional experiments. The possible reasons for this may be

- i) Changes in the relative amount of phases during heating
- ii) removal of the excess oxygen anion vacancies present in the sintered material

Experiments were conducted in which the sintered samples were reheated in air at 800°C upto 5 hours. No measurable change in the relative amounts of the phases was observed. However, the lattice parameters were found to increase slightly as shown in Table 5.1. Also all the samples changed in colour from black to white. The peak in conductivity therefore does not seem to be due to any destabilization of the cubic phase. The second possibility i.e. that the excess anion vacancies introduced due to sintering in oxygen-less atmosphere are removed during conductivity measurement and result in a drop in conductivity is much more likely. That such removal of the anion vacancies is taking place is supported by the change in colour and the increase in lattice parameter observed on heating in air at 800°C . The colour of the samples used for conductivity measurement were also found to become less black after the experiment though they did not become completely white.

83988

Table 5 1

Lattice constants of samples reoxidised in air at 800 °C for 5 hours

Composition	Lattice constant (Å)
C ₀	5.092
C ₄	5.111
C ₈	5.117
C ₁₅	5.129

The temperature at which the peak occurs and also the width of the peak increases with increase in the amount of calcia. From the point of view of anion vacancy removal mechanism this can be rationalised as follows. The diffusion of anion vacancies which is necessary in order that they may migrate to the surface and be removed, will be more difficult as the number of calcium ions increases, as explained by Tien and Subbarao [23]. Moreover the binding energy of the anion vacancy in the lattice will tend to have a wide distribution when calcium ions are added because the vacancy can now have for its neighbours either all zirconium ions or zirconium and calcium ions in varying ratio. This distribution in the binding energy is expected to become broader as the CaO content is increased. This may be the reason for the broadening of the conductivity peaks with increasing calcia content.

Table 5 2
Activation energy

Composition	Activation energy (ev)	
	Before peak	After peak
C ₀	0 7178	0 39
C ₄	1 23	0 31
C ₈	0 1957	-
C ₁₅	0 45	-

Although the reduction in the number of oxygen ion vacancies seems to be a likely mechanism for the peaks in conductivity, further experiments are necessary to establish this

The value of conductivity at low temperature is found to increase as the CaO content is increased from 0 to 8 mole % and then decreases for 15 mole % CaO. This is in agreement with the observation reported in literature.

The activation energies before and after the peak are listed in Table 5 2. If the value for C₄ is ignored, the values follow the trend reported by Tien and Subbarao. The microstructure of C₄ for some unaccounted reason is drastically different than that for the other composition which may be the reason why this discrepancy in the value of activation energy has occurred.

CHAPTER VI

DENSITY AND POROSITY MEASUREMENTS

VI.1 Green Density

The densities of the as pressed samples of each composition were calculated from the following relation

$$\rho_G = \frac{M}{V}$$

where M and V are the mass and volume of the as pressed samples respectively

VI.2 Sintered Density

The as sintered samples were dried in an oven at 150°C in order to remove the moisture or any trapped gaseous materials. The initial dry weight (W_1) of the samples were taken with a SARTORIOUS 2006 MP electronic balance. The samples were then immersed in a beaker containing xylene and placed under a vacuum of about 10^{-2} torr for an hour in order to allow xylene to enter into the pores of the samples by replacing the trapped air bubbles within them. The samples were removed and blotted gently with a tissue paper and the saturated weight (W_2) in air was taken. The samples were then suspended in water and their suspended weight (W_3) were taken. The sintered density was calculated from the following relation

$$\rho_s = \frac{W_1}{W_2 - W_3}$$

The percentage of open porosity was calculated from the following relation

$$\% \text{ open porosity} = \frac{W_2 - W_1}{W_2 - W_3} \times 100$$

VI.3 True Density

The samples were ground to fine powder so that they pass through a 160 mesh sieve and dried in an oven at 150°C. The weight of a clean dry pycnometer was taken. The pycnometer was filled with enough sample such that it is slightly more than quarter-full and its weight W_2 was taken. The pycnometer was filled to its one half volume with distilled water and was boiled in a water bath for an hour. After the pycnometer was cooled, it was filled completely with distilled water and the stopper was inserted. The exterior was wiped dry and care was taken to see that no sample fell out of the pycnometer throughout the test. The weight W_3 of the pycnometer and its contents was taken. The sample was discarded, the pycnometer was cleaned thoroughly and dried and filled completely with distilled water and its weight (W_4) was taken. The specific gravity was obtained from the following relation

$$\text{Specific gravity} = \frac{W_2 - W_1}{(W_4 - W_1) + (W_2 - W_3)}$$

True density $\rho_T = \text{specific gravity} \times (\rho_w - \rho_a)$

where ρ_w and ρ_a are the densities of water and air respectively at the temperature at which the test was performed.

$$\% \text{ true porosity} = \frac{\rho_T - \rho_S}{\rho_T} \times 100$$

$$\% \text{ closed porosity} = \% \text{ true porosity} - \% \text{ open porosity}$$

The densification parameter D was found from the following relation

$$D = \frac{\text{Sintered density} - \text{Green density}}{\text{True density} - \text{Green density}} \times 100$$

Furthermore, the theoretical density of the compositions C_4 , C_8 and C_{15} were calculated using the standard values of theoretical densities of ZrO_2 and CaO in the following manner

Let the theoretical density of A = x gms/cc and B = y gms/cc respectively

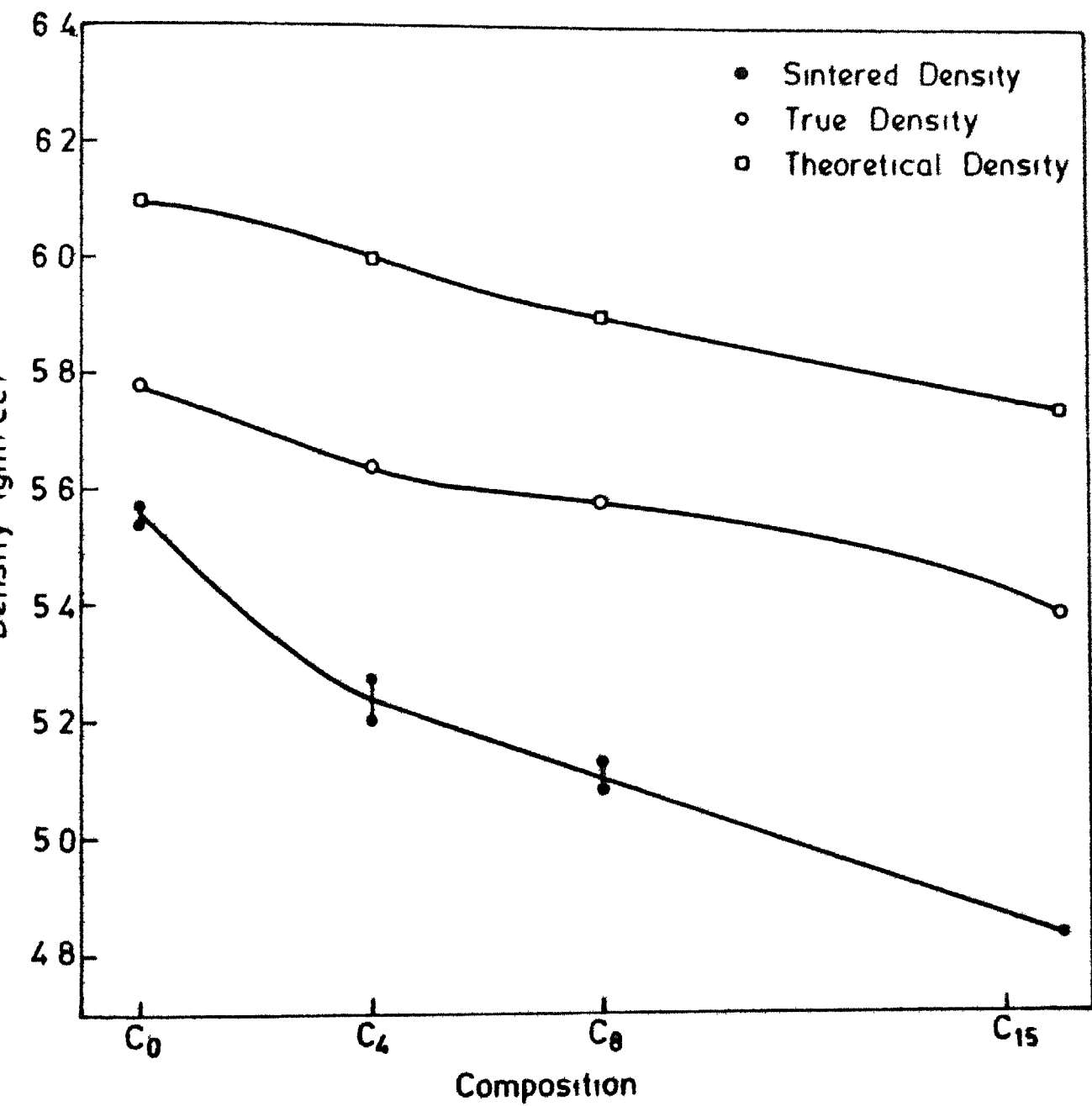
Let the mixture be composed of a and b weight % of A and B respectively. The theoretical density of the mixture is

$$\rho_{TH} = \frac{100 \ xy}{ay + bx}$$

The theoretical density was calculated in order to compare the results of sintered density obtained in the present work.

VI.4 Results and Interpretations

Figure 6.1 shows the variation of sintered density, true density and theoretical density with composition. It is observed that the composition C_0 , which is devoid of calcia possesses the maximum sintered density. There is a steady decrease in the sintered densities as the calcia



6.1

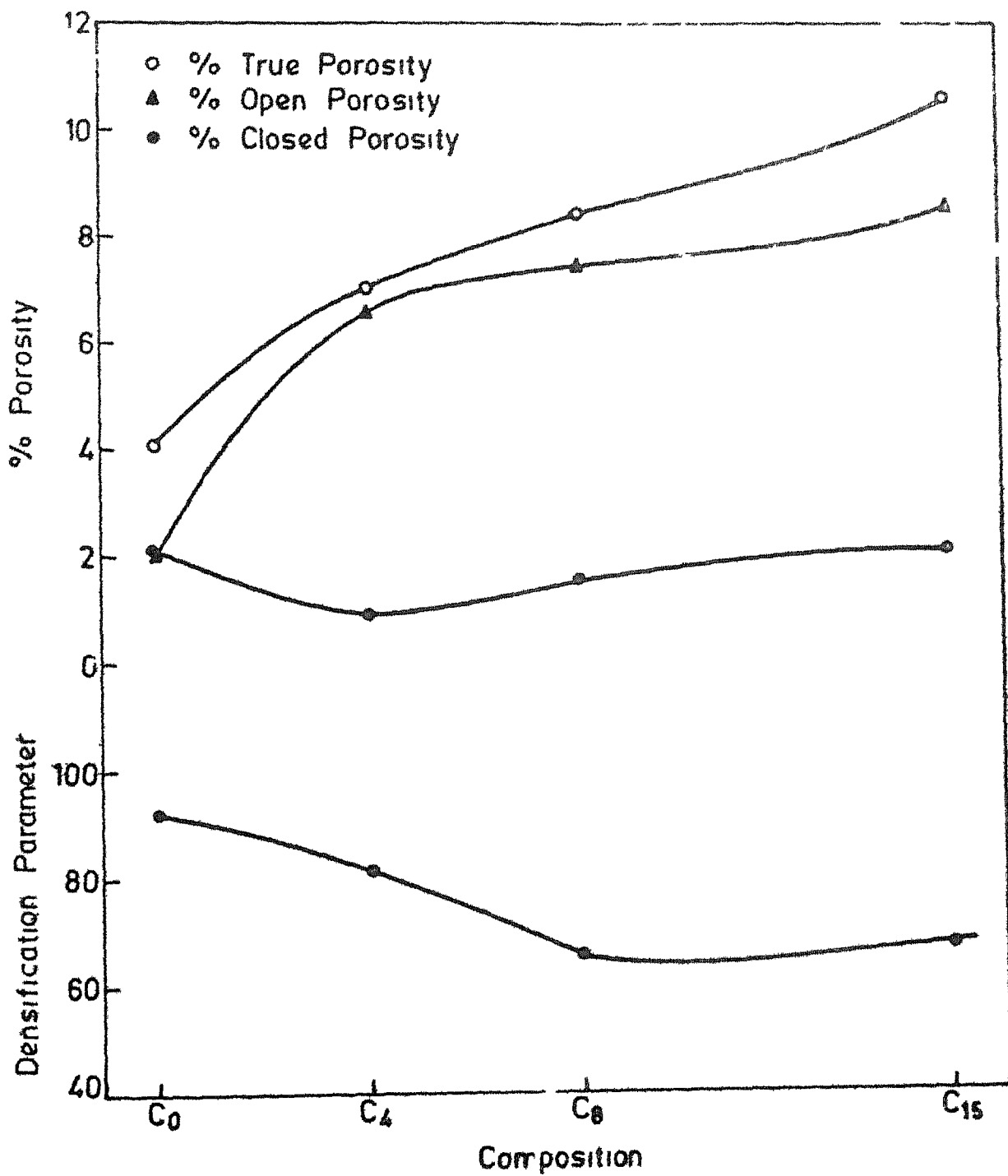
Variation of sintered, true and theoretical density with composition

content in the composition increases. Thus sintered density of $C_0 > C_4 > C_8 > C_{15}$. This is true also in the case of true density as well as the theoretical density as seen from the figure. Comparing the three plots it is seen very clearly that the sintered, true and theoretical densities decrease with increase in calcia content. This may be explained by considering the mass and volume of the unit cell.

On addition of calcia to ZrO_2 , there is a replacement of Zr^{4+} by Ca^{2+} and oxygen ion vacancies are formed in order to maintain charge neutrality. The oxygen ion vacancies increase with addition of calcia resulting in a contraction of the lattice and hence there is a reduction in the volume of the unit cell. This is partly compensated by the size of Ca^{2+} (0.99 \AA) which has replaced Zr^{4+} (0.78 \AA). Ca^{2+} is approximately 25% larger than the Zr^{4+} .

There is considerable reduction in the mass of the unit cell. Since the atomic weight ^{of} calcium is about 55% less than that of zirconium there is a definite loss of weight in the unit cell. This is also supported by the weight loss due to expulsion of oxygen ion from the lattice. Hence there is an overall decrease in the density. As the calcia content increases, the oxygen deficiency correspondingly increases; the density of the composition decreases on increasing the calcia content.

The variation of % open porosity and true porosity with composition is shown in Figure 6.2. Both the



factors increase with increase in calcia content in the composition. The variation of Densification parameter with composition is also shown in the same figure which shows the relative amount of densification attained by a composition on sintering.

CHAPTER VII

CHANGES ON REOXIDATION

VII 1

Oxygen deficiency is induced in ZrO_2 by high temperature sintering in either inert atmosphere or vacuum. Harold Garrett and Robert Ruh [10] report that sintering of ZrO_2 specimen in a vacuum induction furnace at $2300^\circ C$ for three hours operating at 10^{-4} torr or lower resulted in sound, black oxygen deficient zirconia. It was reported by Weber, Garrett, Mauer and Schwartz [13] that ZrO_2 bars sintered in a tantalum resistance vacuum furnace at $2000^\circ C/20$ hrs became black oxygen deficient samples and air annealing at high temperature $\approx 1000^\circ C$ led to their rapid oxidation and consequent disintegration. The blackness of zirconia heated in vacuo at temperature $> 2100^\circ C$ was attributed to the solid solution of zirconium in zirconia. Carniglia et.al. [11] studied the lattice volume and thermal expansion of the unit cells of ZrO_{2-x} and ZrO_2 by X-ray diffraction. They report that in both monoclinic and tetragonal ZrO_2 , the volume of the O deficient material was slightly less than that of the stoichiometric material. They also determined the value of x in the formula ZrO_{2-x} by finding the weight change in a sample reheated to constant weight at $1000^\circ C$.

In keeping the above results in mind, the as sintered samples were subjected to reoxidation in air at

different temperatures. The effect of reoxidation on the crumbling behaviour, weight gain and lattice parameter was studied.

VII 2 Experimental Procedure

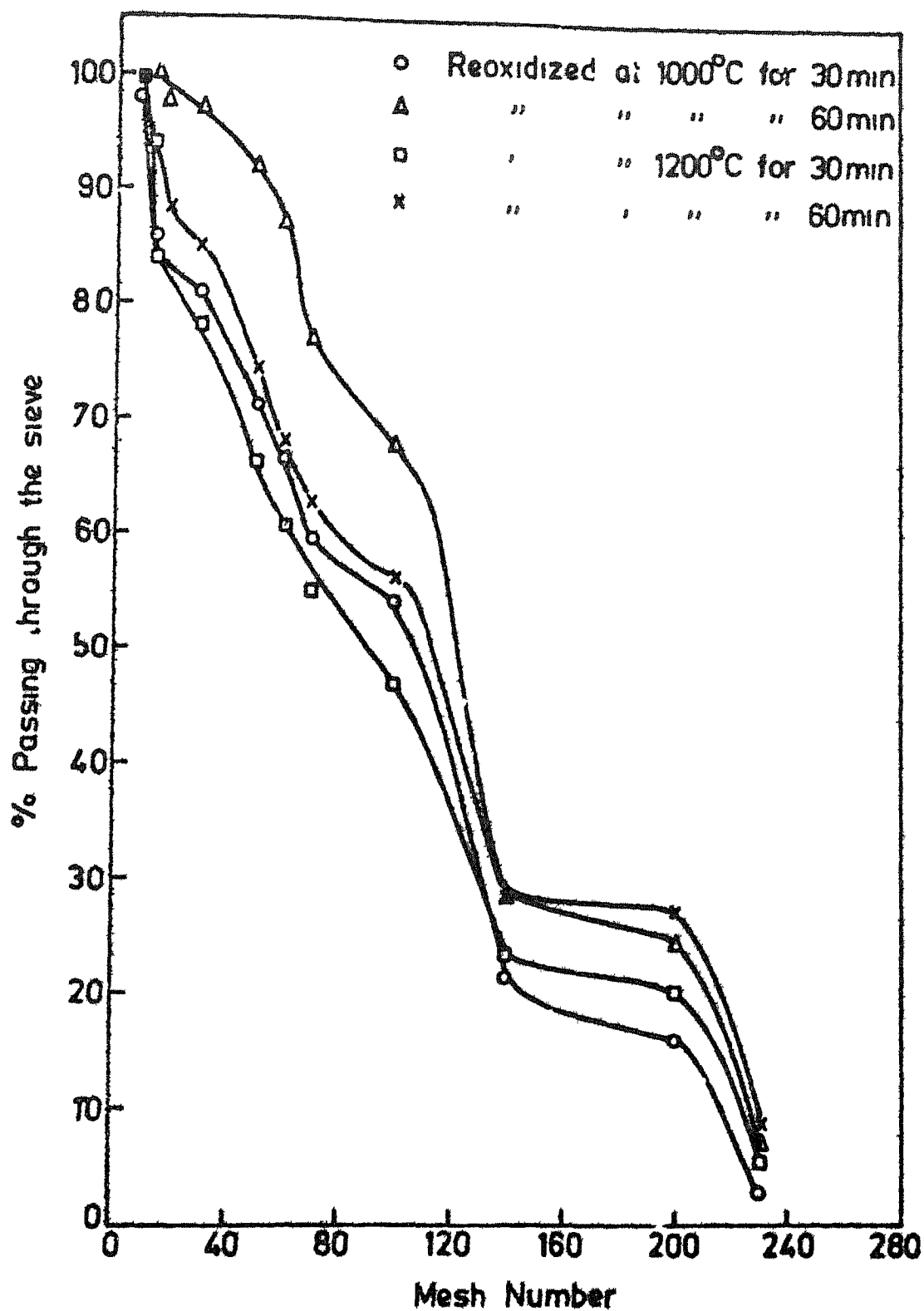
VII 2 1 Weight change on reoxidation

A small alumina crucible was cleaned thoroughly with acetone, distilled water, dil. HCl and finally heated to 1000°C to remove all volatile material. The crucible was weighed (W_1) with a SARTORIOUS-2006 MP electronic balance to an accuracy of 10^{-4} grams. A piece of the sample was kept in the crucible and the weight (W_2) was taken. The crucible and contents were placed in a globar furnace at 1300°C for a few minutes, removed from the furnace and the weight (W_3) was again taken. The procedure of heating at constant temperature for further time was repeated till there was no more gain in weight.

VII.2.2 Crumbling behaviour

Another batch of samples were heated at 1000°C for 12 hours and 1350°C for 15 hours respectively. Their crumbling behaviour was studied by crushing the reoxidized samples by finger pressing and performing the sieve analysis.

The X-ray diffraction analysis of the reoxidized samples have been discussed earlier which showed an increase in the lattice parameter. Figure 7.1 shows the % of particles passing through sieves of different mesh numbers as function of reoxidation at different temperatures and times. It is seen that fineness of particles increases on reoxidation at 1000°C.



7.1

% variation of sample passing through sieve with mesh number as a function of different temperatures and time

VII 3 Results and Interpretation

The maximum weight change on oxidation upon heating at 1300°C is shown in Figure 7.2

It is seen from this figure that there is an increase in the percentage weight gain on reoxidation with increasing calcia content. This increase in weight can be due to the substitution of the excess anion vacancies by oxygen ion from air as well as due to the oxidation of the zirconium metal to ZrO_2 in C_8 and C_{15} .

Since a unit cell of cubic zirconia contains 4 atoms of Zr and 8 atoms of oxygen, the density is given by

$$\rho_1 = \frac{M}{V} = \frac{1}{a^3} \left(\frac{4A_{Zr}}{N} + \frac{8A_O}{N} \right)$$

where A_{Zr} , A_O = Atomic weights of zirconium and oxygen respectively

a = Lattice constant

N = Avogadro number.

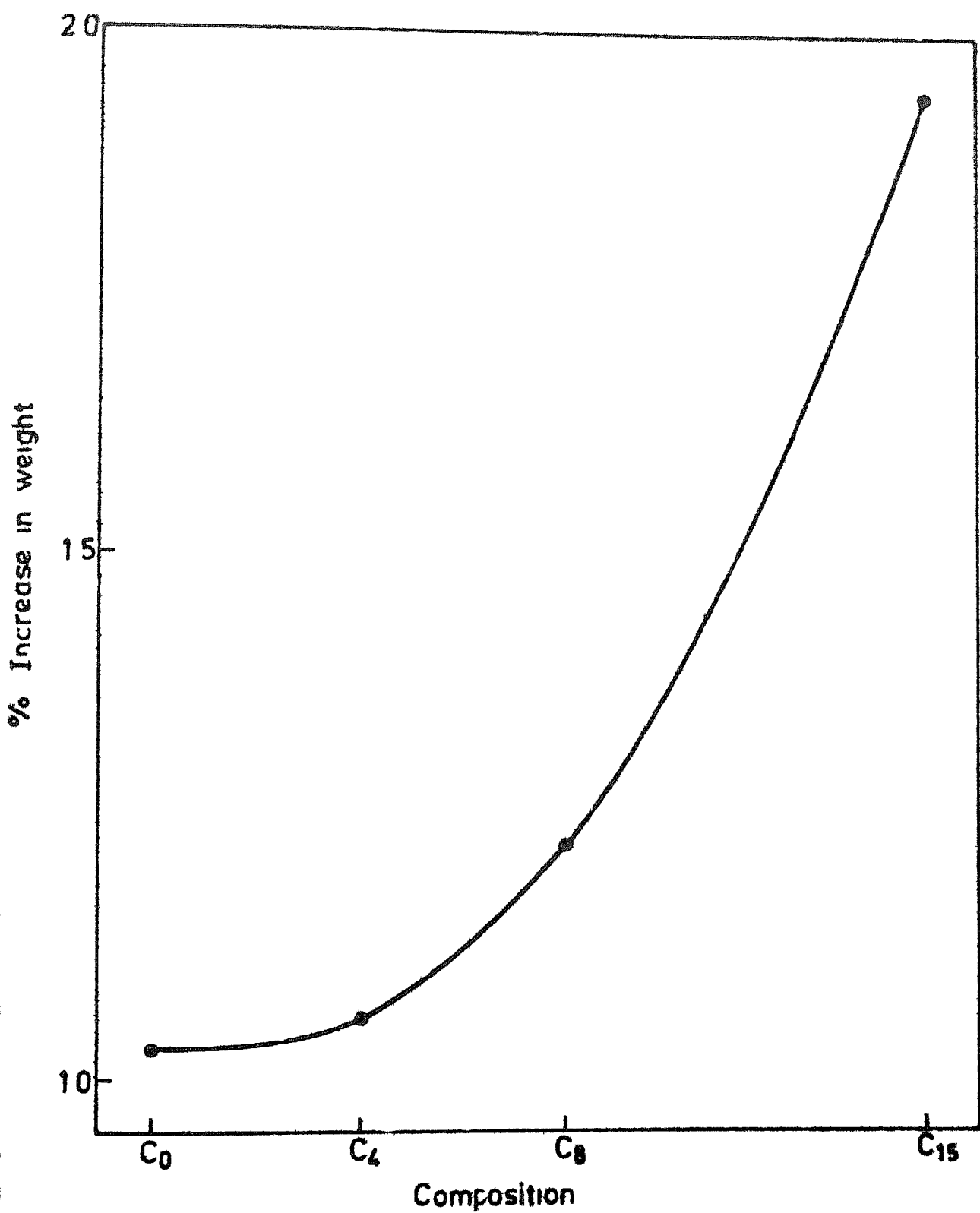
On addition of X mole % of calcia, the density is

$$\rho_2 = \frac{1}{a^3} \frac{4(1 - \frac{X}{100}) A_{Zr} + 4 \frac{X}{100} A_{Ca}}{N} + \frac{8(1 - \frac{X}{100}) A_O}{N}$$

because X mole % of anion vacancies are also created, where A_{Ca} = Atomic weight of calcia.

Let $y\%$ be the total vacancies in a sample containing X mole % calcia upon sintering in oxygen deficient atmosphere. The density ρ_3 is then

$$\rho_3 = \frac{1}{a^3} \frac{4(1 - \frac{X}{100}) A_{Zr} + \frac{4xA_{Ca}}{100}}{N} + \frac{8(1 - \frac{y}{100}) A_O}{N}$$



where ρ_3 is the true density of the composition containing x mole / of calcia

The excess concentration of vacancies due to sintering in oxygen deficient atmosphere is

$$\Delta = Y - X$$

From the value of ρ_3 and lattice parameter determined experimentally on sintered samples after powdering, Y and Δ are calculated as above and are given in Table 7.1

Table 7 1

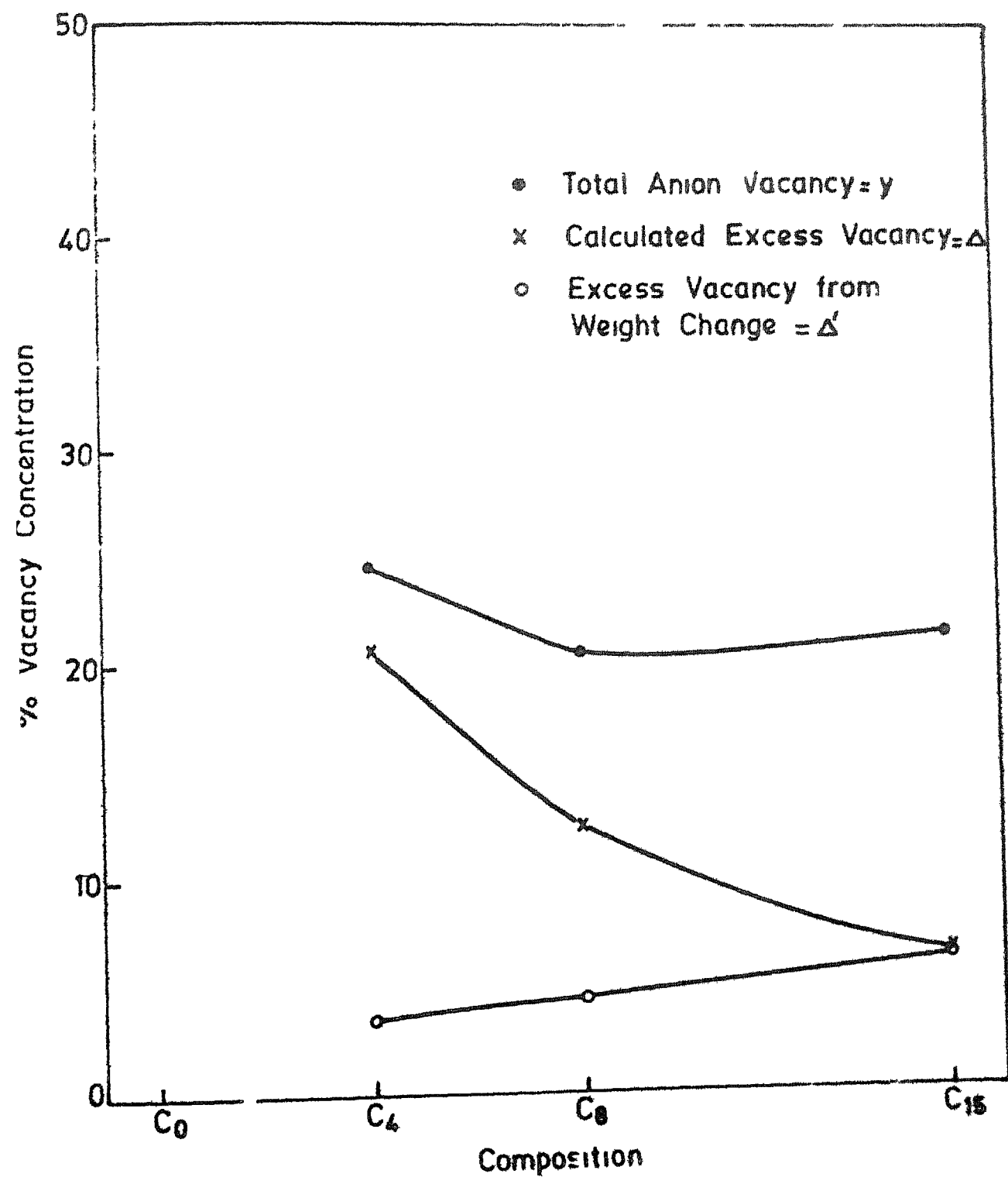
x	ρ_3	Y	Δ	Δ'
0	5.78	-	-	-
4	5.64	24.61	20.61	3.73
8	5.58	20.55	12.55	4.30
15	5.36	21.25	6.25	6.59

If it is assumed that all the weight increase upon oxidation is due to removal of excess anion vacancies, then the concentration of excess vacancies is given by

$$\Delta_1 = \frac{\rho_3 a^3 N x}{8A_o} \quad (\text{Appendix) 7.1}$$

where ρ_3 = True density

a = Lattice parameter before oxidation



N = Avogadro's number

x = % weight gain

A_O = Atomic weight of oxygen

Values of Δ' calculated according to the equation 7.1 are also listed in Table 7.1 and plotted in Figure 7.3 together with Y and Δ

From the figure it can be said that,

- (1) The number of excess anion vacancies created due to sintering in oxygen deficient atmosphere decreases with increase in calcia content
- (2) The difference between Δ and Δ' suggests that all the excess vacancies created during sintering are not removed during reoxidation. Much more careful measurements of density are needed to verify this result

CHAPTER VIII

MECHANICAL PROPERTIES

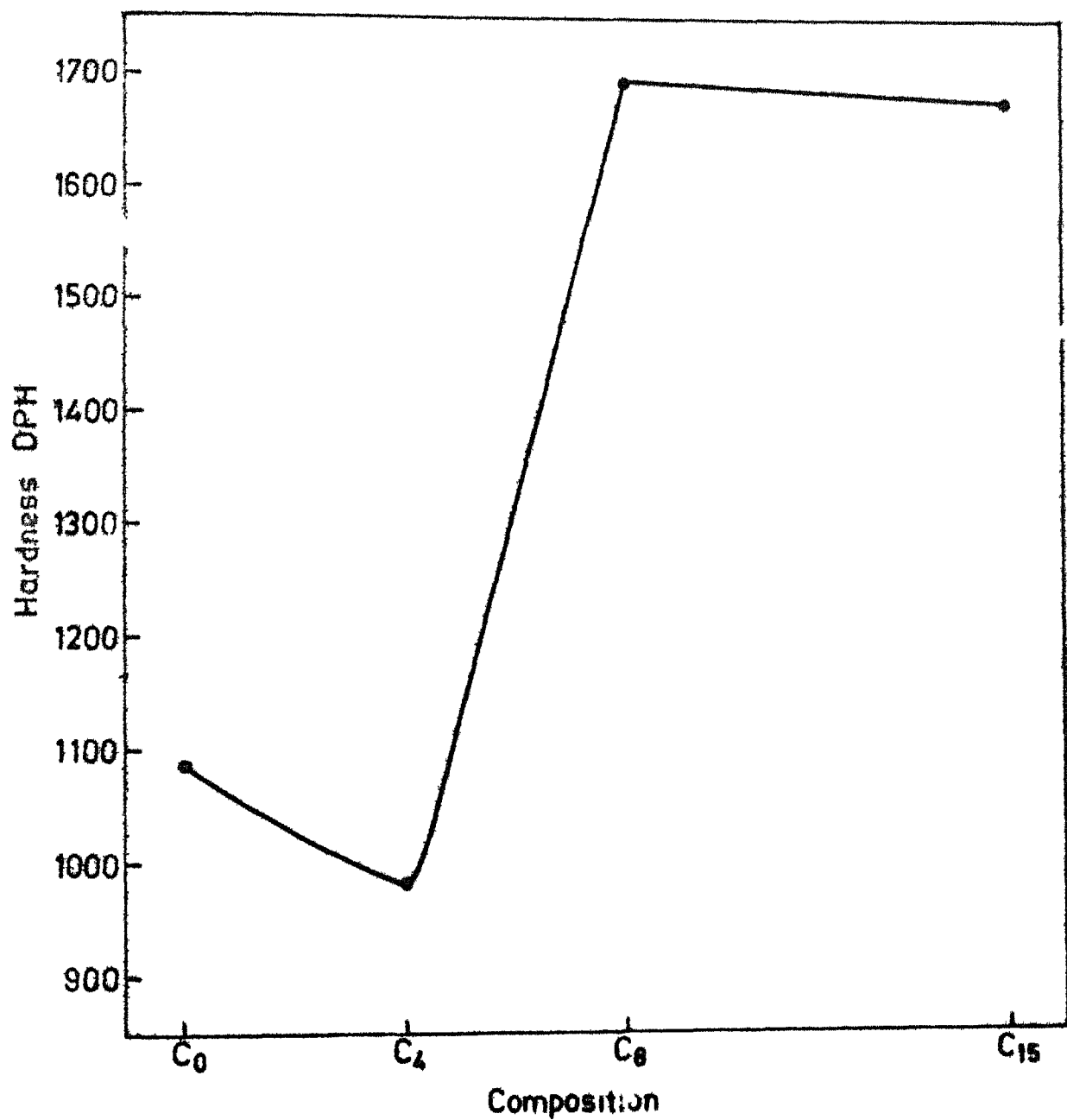
All the three parameters i.e. microhardness, Young's modulus and modulus of rupture play an important role in the characterization of a ceramic material with regard to its application as a refractory material. A brief study of these parameters was made and is reported here.

VIII 1 Microhardness

Microhardness was measured with a Vicker Pyramidal indenter on a LEITZ MINILOAD 2 microhardness instrument. The samples were polished in the same manner as was done for microstructure analysis by SEM discussed earlier. They were mounted on an aluminium stub by epoxy resin. A load of 100 grams was applied to make measurements for all compositions. The indents were made within the grains of C_0 and C_4 . Since the microstructure of C_8 and C_{15} was not clearly visible, it was not possible to distinguish whether the indents were made within the grain or at the grain boundary. Studies were made on a large number of samples and on different regions.

The variation of microhardness with composition is shown in Figure 8.1 1.

It is observed that the Vickers Pyramid hardness value of C_0 and C_4 are close to 1000 whereas those of C_8 and C_{15} are close to 1700. This is in agreement with the



8 1 1 Variation of hardness with composition

report of King and Vavorsky [24] They found the microhardness of zirconia-magnesia system to vary between 1300 and 1800 DPH for an addition of MgO between 2.8 and 5.8 wt %. They also report that the hardest material were brittle and tended to fracture during testing. Swain and co-workers [25] found the hardness of cubic phase of magnesia stabilized zirconia to be much more than the monoclinic phase. They report the hardness of cubic phase to be 1375° DPH (13.5 GPa) and monoclinic phase to be 745° DPH (7.3 GPa). They explained this hardness between the two phases on the basis of the substantial hardness anisotropy and by the evidence for deformation twinning about the hardness impression displaced by monoclinic crystal.

Another reason for the high value of hardness of C_8 and C_{15} may be the strained lattice produced by the large number of anion vacancies in the compositions as discussed earlier.

It may be mentioned here that the indents did not form any cracks in the case of C_0 and C_4 whereas fine and distinguishable cracks were formed at the edges of the indent in C_8 . In the case of C_{15} , the indent formed a damaged region around itself at this load. This indicates that C_0 and C_4 have higher fracture toughness than C_8 and C_{15} . This agrees with the well known advantage of partially stabilized zirconia over the fully stabilized zirconia with respect to fracture toughness and thermal shock resistance.

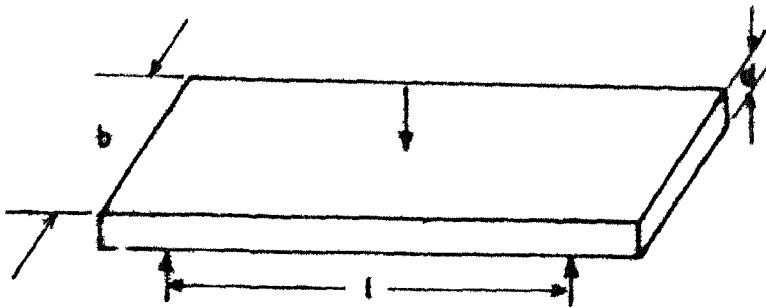
VIII 2 Youngs Modulus and Modulus of Rupture (MOR)

The MOR was found using the three point bending method (Figure 8 2 1) Thin samples of size approximately $1.5 \times 0.2 \times 0.1$ cm were ground and polished with 100, 240 and 400 grit size silicon carbide powder on a glass plate. It was not possible to make samples of required dimensions from composition C_4 due to presence of macrocracks. The MOR of the samples of C_0 , C_8 and C_{15} was found out using an INSTRON 1195 SYSTEM. A 1000 Kg load cell was used with a cross head speed of 0.05 mm/min. The span used in three point bending is 6 mm and three specimens of composition were tested. Table 8 2 1 shows the variation of MOR with the composition. C_8 and C_{15} possesses relatively higher values of MOR and Youngs modulus compared to that of C_0 . It is seen that the MOR values of all compositions studied are considerably less than the reported values in literature (MOR \sim 200 MPa, E \sim 170-240 GPa) [26]. However the values are considerably better than those obtained earlier on samples which were prepared in a similar way but sintered in air [27].

Table 8 2 1

Values of MOR and Youngs modulus for different compositions

Parameter	Composition		
	C_0	C_8	C_{15}
MOR (MPa)	16.05, 21.12, 80.52 13.54	41.48, 74.34, 62.44, 66 51.09	
Youngs modulus (GPa)	2.32, 2.98, 11.34, 0.77	28.15, 39.07	4.47, 5.1



Modulus of Rupture MOR

$$= \frac{3}{2} \times \frac{\text{Load (Kg)} \ l}{10^2 \times b \cdot d^2} \text{ MPa}$$

Young's modulus E

$$= \frac{\text{Load (Kg)} \ l^3}{4 \times 10^2 (\text{deflection}) b d^3} \text{ MPa}$$

(All dimensions in centimeters)

8 2 1

Determination of MOR and Youngs modulus by
three point bending method

CHAPTER IX

CONCLUSIONS

To study the effect of sintering in an oxygen deficient atmosphere on ZrO_2 with CaO , analysis were done on phases, microstructure, density, conductivity, mechanical properties and reoxidation behaviour

ZrO_2 specimens with 0, 4, 8 and 15 mole % of calcia were sintered at 1900°C in a nitrogen gas atmosphere at $P_{\text{O}_2} = 3 \times 10^{-10}$ atmosphere. All the samples were either black or grey in colour indicating O deficiency

X-ray analysis showed that sintering in a highly oxygen deficient atmosphere has a stabilizing effect on the samples similar to that of addition of calcia. C_0 samples (containing no calcia) were found to have 30% of cubic phase and the composition C_8 was completely stabilized in the defect fluorite structure. A shrinkage in the volume of the lattice is indicated by comparatively lower values of lattice constants. Reoxidation in air caused destabilization which is found to be easier at 1000°C than at 1350°C . This is expected since the tetragonal \rightleftharpoons monoclinic transformation temperature is at about 1000°C . An increase in the lattice parameter values on reoxidation indicated volume expansion due to reentry of oxygen in the lattice.

Transmission electron microscopy indicated the presence of metallic zirconium in samples of C_8 and C_{15} .

The microstructure of samples containing 4 mole % calcia is found to be entirely different from those of C_0 , C_8 and C_{15} . The exact reason for this is not known. The samples of C_8 and C_{15} contained metallic zirconium in the form of discrete white particles concentrated in the pores, the concentration of which were more near the edges of the sample.

Conductivity of samples containing 0, 4 and 8 mole % calcia respectively was found to increase with increase in temperature, reach a maximum and then drop before rising again with further increase in temperature. It has been suggested that this may be a result of removal of the excess oxygen ion vacancies. If we ignore the value of activation energy of C_4 , it is seen that the activation energy reduces on increase in amount of calcia till composition C_8 is reached and then decreases on further increase in addition of calcia as seen in the case of C_{15} . This is in agreement with the literature.

Density measurements indicate that the sintered density of samples decreases with increasing amount of calcia. The same behaviour is seen on measurement of true density. This may be explained on the basis of change in the mass and volume of a unit cell due to replacement of Zr^{4+} ion by smaller and lighter Ca^{2+} and also oxygen ion vacancies.

The open and closed porosity increase with increase in addition of calcia. Further experiments are required to explain this result.

Studies on reoxidation behaviour of samples indicated that all of them became white in colour on reoxidation at $\geq 1000^\circ\text{C}$. The increase in weight of the samples on reoxidation at 1300°C has been measured. It is seen that the % weight gain increases with increase in addition of calcia.

An interesting feature noticed is that samples reoxidized at 1300°C for 2 hours retained their shape and integrity while all compositions except C_{15} on reoxidation at 1000°C crumble to fine particles. This is suggested to be due to disintegration being predominant at the monoclinic \rightleftharpoons transformation temperature.

The microhardness as well as the MOR and Young's modulus of the composition C_8 and C_{15} are distinctly higher than that of C_0 . This may be partly because the cubic phase is much harder than the monoclinic phase and partly because of the hardness effect of the excess anion vacancies.

REFERENCES

- 1 Weber, Garrett, Mauer and Schwartz, "Observation on the stabilization of zirconia" J Amer Ceram Soc , 39(6), 197-207 (1956)
- 2 John D. Buckley and H H Wilson, "Destabilization of zirconia by cyclic heating". J. Amer Ceram Soc , 46(10), 510 (1963)
- 3 G K Bansal and A H Heuer, "Precipitation in partially stabilized zirconia". J Amer Ceram Soc , 58(5-6), 235-238 (1975)
- 4 R C Garvie, "The cubic field in the system CaO-ZrO_2 " J Amer Ceram Soc , 51, 553-556 (1968)
- 5 Kohei Kodaira, Yushiro Iwasaki and Toru Matsushita, "Stabilization of zirconia under high pressure" J Amer Ceram. Soc , 59, 183-184 (1976).
- 6 R C Garvie and Patrick S Nicholson, "Structure and thermomechanical properties of partially stabilized zirconia in the CaO-ZrO_2 system". J Amer. Ceram Soc., 55, 152-157 (1972)
- 7 D L Porter and A.H Heuer, "Mechanisms of toughening PSZ". J. Amer. Ceram. Soc , 60(3-4), 183 (1977).
8. P D Johnson, "Behaviour of oxides and metals alone and in combination in vacuo at high temperature" J Amer Ceram Soc., 33, 168-171 (1950)
- 9 L L Fehrenbacher and L A Jacobson, "Metallographic observation of monoclinic-tetragonal phase transformation in ZrO_2 " J Amer. Ceram. Soc., 48(3), 157-161 (1965)
- 10 Harold Garrett and Robert Ruh, "Fabrication of specimens from pure dense oxidized zirconia" Amer Ceram. Soc. Bull , 47(6), 578-579 (1968)
- 11 Carniglia, Brown and Schroeder, "Phase equilibria and physical properties of O-deficient zirconia and thorium". J Amer. Ceram. Soc., 54(1), 13-17 (1971).
12. Robert Ruh, Norman Tallan and Harry Lipsiff, "Effect of metal additions on microstructure of zirconia", J Amer. Ceram Soc , 47(12), 632 (1964)
13. Weber, Garrett, Mauer and Schwartz, J Amer. Ceram. Soc., 39(6), 197 (1956).

- 14 Walter Tripp and Norman M Tallan, "Revised weight change in nonstoichiometric ZrO_2 " J Amer Cer Soc., 55(2), 60 (1972)
- 15 Darken and Gurry, "Physical chemistry of metals". McGraw-Hill, 1953
- 16 Pol Duwez and Francis Odell, "Quantitative analysis of monoclinic zirconia by X-ray diffraction" J Amer Ceram Soc , 32(5), 180-183 (1949)
- 17 J Adams and B Cox, "Irradiation induced phase transformation in zirconia solid solution". J Nucl. Energy, Part-A, 11(1), 31 (1959)
- 18 R C Garvie and P S Nicholson, "Phase analysis in zirconia systems" J Amer Ceram Soc , 55, 303-305 (1972)
19. Fanawalt powder diffraction file for inorganic compounds.
- 20 Charles S Barrett and T B Massalski, "Structure of metals" McGraw-Hill Inc , 144-145
21. Robert Ruh and Harold J Garrett, "Nonstoichiometry of ZrO_2 and its relation to tetragonal-cubic inversion in ZrO_2 " J Amer Ceram. Soc., 50(5), 257-261 (1967).
- 22 Anil V Virkar and D Lynn Johnson, "Wetting characteristics of Zr with ZrO_{2-x} " J Amer Ceram. Soc , 85 (Jan. Feb. 1977)
- 23 Tien and E C Subbarao, "X-ray and electrical conductivity study of fluorite phase in system ZrO_2 -CaO" J Chem. Physics, 39, 1041 (1963).
- 24 Alan G Kind and Paul J Vavorsky, "Stress relief mechanisms in magnesia and stabilized zirconia". J Amer Ceram Soc , 57, 38-42 (1968)
- 25 Michael V Swain, R C Garvie and Richard H.J Hannik, "Influence of thermal decomposition on the mechanical properties of magnesia stabilized cubic zirconia" J Amer Ceram Soc , 66(5), 358-362 (1983)
- 26 Creyke, Sainsbury and Morrell, "Design with non-ductile materials". Applied science Publishers, London (1982).
- 27 R Gopalakrishnan, "Effects of CaO and TiO_2 additives on sintering and microstructure of zirconia" M.Tech. Thesis, I.I.T Kanpur (1982)

APPENDIX

CALCULATION FOR / VACANCY CONCENTRATION FROM / WEIGHT GAIN

$$\% \text{ weight gain} = x$$

$$\text{Weight change for 1 gram} = \frac{x}{100} \text{ grams}$$

$$\text{Let, } n = \text{Number of atoms entering } 0.0x \text{ gram}$$

$$n = \frac{N}{A_o} \frac{x}{100}$$

$$\text{Volume of 1 gram after reoxidation} = \frac{1}{\rho_1} \frac{a_2^3}{a_1^3}$$

$$\text{Number of oxygen entering 1 cc} = \frac{\rho_1 a_1^3}{a_2^3} \cdot n$$

$$\text{Number of oxygen entering } a_2^3 = \rho_1 a_1^3 n$$

$$\% \text{ vacancy filled by them} = \frac{\rho_1 a_1^3 n}{8} \times 100$$

$$= \frac{\rho_1 a_1^3 N x}{8A} \%$$